

Review

3D Printing Technologies in Biosensors Production: Recent Developments

Giulia Remaggi , Alessandro Zaccarelli and Lisa Elviri * 

Food and Drug Department, University of Parma, Parco Area delle Scienze 27/a, 43124 Parma, Italy; giulia.remaggi@unipr.it (G.R.); Alessandro.zaccarelli@studenti.unipr.it (A.Z.)

* Correspondence: Lisa.Elviri@unipr.it; Tel.: +39-0521-905087

Abstract: Recent advances in 3D printing technologies and materials have enabled rapid development of innovative sensors for applications in different aspects of human life. Various 3D printing technologies have been adopted to fabricate biosensors or some of their components thanks to the advantages of these methodologies over the traditional ones, such as end-user customization and rapid prototyping. In this review, the works published in the last two years on 3D-printed biosensors are considered and grouped on the basis of the 3D printing technologies applied in different fields of application, highlighting the main analytical parameters. In the first part, 3D methods are discussed, after which the principal achievements and promising aspects obtained with the 3D-printed sensors are reported. An overview of the recent developments on this current topic is provided, as established by the considered works in this multidisciplinary field. Finally, future challenges on the improvement and innovation of the 3D printing technologies utilized for biosensors production are discussed.

Keywords: 3D printing technologies; biosensors; electrochemical biosensors; material extrusion; vat photopolymerization; material jetting; analytical detection



Citation: Remaggi, G.; Zaccarelli, A.; Elviri, L. 3D Printing Technologies in Biosensors Production: Recent Developments. *Chemosensors* **2022**, *10*, 65. <https://doi.org/10.3390/chemosensors10020065>

Academic Editor: Núria Serrano

Received: 17 December 2021

Accepted: 4 February 2022

Published: 7 February 2022

Publisher's Note: MDPI stays neutral with regard to jurisdictional claims in published maps and institutional affiliations.



Copyright: © 2022 by the authors. Licensee MDPI, Basel, Switzerland. This article is an open access article distributed under the terms and conditions of the Creative Commons Attribution (CC BY) license (<https://creativecommons.org/licenses/by/4.0/>).

1. Introduction

Three-dimensional (3D) printing was born in 1986, with the publication of Chuck Hull's patent [1], who invented stereolithography; from here it has evolved and differentiated, with the introduction of new printing techniques and numerous materials with different characteristics. Currently 3D printing, also known as “additive manufacturing” (AM) or rapid prototyping, is advancing in both the industrial and academic sectors for its potential to address several important challenges [2,3]. Digital files deriving from a magnetic resonance image, a computer-aided design (CAD), or a computed tomography (CT) scan provide the desired forms that can be accurately manufactured in 3D items by drawing multiple layers of biomaterials [4]. A standard triangle/tessellation file (STL) file is then created from the digital data and allows for the conversion of the object of interest into thinly sliced horizontal cross sections for the successive printing processes based on a layer-by-layer deposition of material [5]. 3D printing is considered one of the most potent opportunities for the manufacture of complex geometries with high precision, rapid prototyping, cost and material savings, flexibility in making object modifications, and personal customization [6]. According to the ASTM F2792 standard [7], AM processes are grouped into seven categories (Figure 1):

- Binder jetting (BJ): in this process a liquid bonding agent is selectively deposited to join powder materials.
- Directed energy deposition (DED): refers to an AM technique known by other names such as laser-engineered net shaping (LENS), direct metal deposition (DMD), electron beam additive manufacturing (EBAM), directed light fabrication, and 3D laser cladding, where thermal energy is used to melt the raw materials in layer-by-layer fashion.

- Material extrusion (ME): refers to a process in which the material is extruded through a nozzle or orifice.
- Material jetting (MJ): refers to the selective deposition of droplets of materials, including photopolymer and wax.
- Powder bed fusion (PBF): refers to an AM method in which regions of a powder bed are fused by thermal energy.
- Sheet lamination (SL): refers to an AM process in which sheets of material are bonded to create the final object.
- Vat photopolymerization (VP): refers to an AM process in which the object is created from a liquid photopolymer in a vat cured by light-activated polymerization.

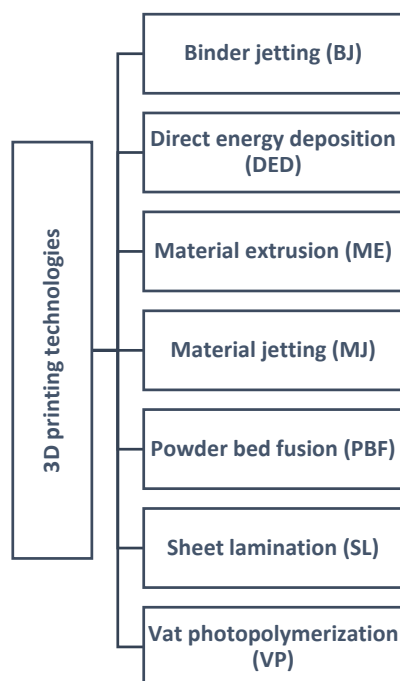


Figure 1. Schematic diagram of the seven different 3D printing technologies according to the ASTM F2792 standard.

Thus, each AM technology presents its own peculiar characteristics in terms of printing time, printing materials, resolution, precision, object dimensions, reduced cost, and use in various applications. Among the different application fields, the world of sensors has seen the importance of 3D printing techniques blossom thanks to the essential advantages of rapid manufacturing above described [3,8,9]. The International Union of Pure and Applied Chemistry (IUPAC) provided the definition of a biosensor as a system that exploits selective biochemical interactions between analytes and specific enzymes, immunosystems, organelles, or whole cells for quantitative purposes, resulting in electrical, thermal, magnetic, or optical signals [10]. The first biosensor was developed in the 1962 by Clark and Lyons to quantify the glucose level in biological samples by electrochemical detection of oxygen or hydrogen peroxide using immobilized glucose oxidase electrode [11,12]. Since then, both the production technologies and applications of biosensors have evolved [13]; however, it is possible to schematize the structure of a biosensor to that shown in Figure 2. In particular, in a typical biosensor four components can be identified [14]:

- Analyte: the species of interest to be identified during the analysis.
- Bioreceptor: the species that selectively recognizes the analyte. Naturally occurring or in vitro expressed molecules such enzymes, cells, aptamers, deoxyribonucleic acid (DNA), or antibodies can be used for the analyte bio-recognition process, generating a detectable signal in the form of light, heat, pH, charge, or mass change, etc.

- Transducer: a device capable of converting the analyte/receptor binding into measurable optical or electrical signals that are usually proportional to the amount or concentration of the analyte.
- Display: the system, such as the liquid crystal display of a computer or a direct printer, that generates the numeric or graphical results of the biosensor analysis.

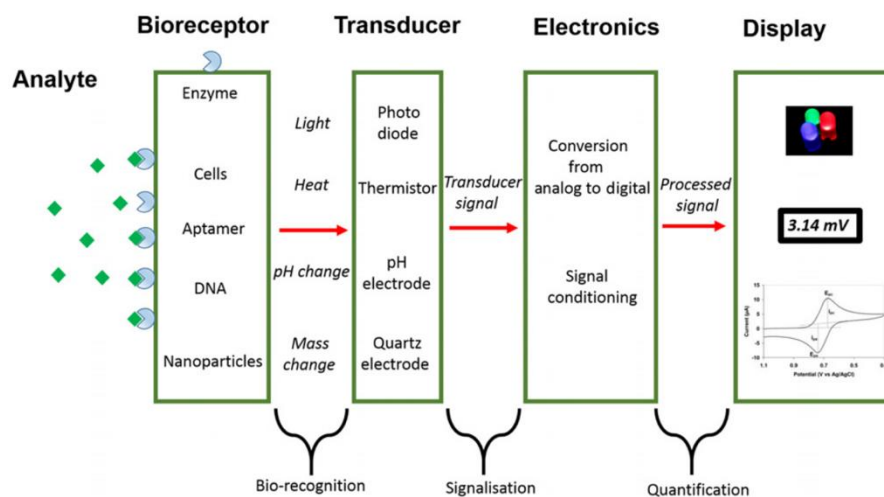


Figure 2. Schematic representation of a biosensor. Reproduced with permission from Bhalla et al. [14], *Essay in Biochemistry*, 60, 1–8. Published by Portland Press, 2016.

Nowadays, the role of biosensors is continuously growing and evolving in the scenario of analytical techniques in order to enable the most challenging analyte detection. In such a context amongst the several manufacturing approaches used in the fabrication of biosensors, 3D printing technologies are successfully used and accepted. Different single biosensor components or even molds to prepare sensors by casting [15], etc., can be manufactured. Considering the materials commonly used in biosensors production, 3D printing techniques are compatible with a variety of materials, such as thermoplastic filaments polylactic acid (PLA) or acrylonitrile butadiene styrene (ABS), and such as graphene or carbon black [16,17]. Thus, thanks to technological advances, 3D-printed sensors have found a significant role in different aspects of human life [5,16–19]. In this review, works published in the last two years (2020–2021) on the 3D printing of biosensors components for different applications are taken into consideration. First, publications were grouped on the basis of the 3D printing technologies used for the production of some biosensor components; then the 3D printing technologies, divided principally according to F2792 standard, are presented based on the principles of operation. The publications thus considered were subsequently evaluated on the basis of application fields, reporting the main analytical challenges and the principal results obtained thanks to the 3D-printed biosensors. With this review, we want to provide an overview of the most recently used 3D printing technologies for biosensors development in multidisciplinary research, highlighting the advantageous role of 3D printing for the realization of devices, over traditional methods such as higher resolution, end-user customization, and rapid prototyping.

2. 3D Printing and Biosensors Production

3D printing technologies offer promising innovation in the manufacturing of biosensors or biosensor components. The most relevant scientific literature dealing with this topic is reported in Table 1. Table 1 provides a summary of the 3D printing technologies used to fabricate biosensors or the parts of a biosensor, the material used for printing, the application field, and the analytical applications. In this review, we grouped publications on the basis of the 3D printing technology used in the biosensor preparation and we discuss them as a function of the application field. The application fields, the principal analytical purposes, and the limits of detection of the analytes investigated in different biological

matrices are reported. The main 3D printing technologies applied in the works considered here are material extrusion (ME), vat photopolymerization (VP), and material jetting (MJ); ME consists principally of fused deposition modelling (FDM), inkjet printing, and aerosol-jet-printed (AJP) methods; VP is based primarily on stereolithography (SLA), while MJ utilizes Multijet technology. Lastly, some examples of other 3D printing technologies for biosensors production such as powder bed fusion and binder jetting, as well as some combined approaches, are listed.

Table 1. 3D printing technologies in biosensors production, their fields of application, and the main analytical purposes. Limits of detection and biological sample of interest are also reported when the information was available in related publications (N/A = not available).

3D Printing Technologies	Field of Application	Analytical Purposes	Limit of Detection	Biological Sample	3D-Printed Materials	Ref.
Material Extrusion: FDM	Biomedical	Hydrogen peroxide detection	11.1 μM	N/A	Graphene/PLA	[20]
Material Extrusion: FDM	Biomedical: wearable sensors	Glucose determination in human sweat	1.2 $\mu\text{mol/L}$	Human sweat	Carbon PLA/TPU	[21]
Material Extrusion: FDM	Biochemical: chiral sensors	Tryptophan enantiomers resolution and quantification	N/A	N/A	PLA	[22]
Material Extrusion: FDM	Biomedical: diagnosis	Anticancer drugs direct quantification	5×10^{-8} M in serum	Human biological fluids	PLA	[23]
Material Extrusion: FDM	Biomedical: point-of-care (POC) diagnostics	DNA amplification (LAMP)	N/A	Human saliva	PP	[24]
Material Extrusion: Inkjet printing	Biomedical	Epithelial cell cultures monitoring	4.36 cell-index unit/cells \times cm^{-2}	Epithelial cells	AgNPs/SU-8	[25]
Material Extrusion: AJP	Biomedical	Cytokine monitoring in bovine serum	IFN- γ : 25 pg/mL; IL-10: 46 pg/mL	Bovine serum	Graphene-nitrocellulose	[26]
Material Extrusion: AJP	Biomedical: diagnosis	SARS-CoV-2 antigens detection	S1 protein: 2.8×10^{-15} M; RBD: 16.9×10^{-15} M	Human biological fluids	AuNPs-PDMS	[27]
Material Extrusion: FDM	Point-of-care diagnostics	Dopamine detection	1.45 $\mu\text{g/mL}$	N/A	CNT/CB/PLA	[28]
Material Extrusion: FDM	Biomedical: epithelial cancer biomarkers detection	Mucin 1 quantification	80 nM	Breast cancer cells	Nanocarbon-PLA	[29]
Material Extrusion: DLP	Biomedical: multiplexed protein biomarker ELISA	IL-6, CRP, CEA, PSA	IL-6: 1.75 pg/mL; CRP: 26 pg/mL; CEA: 7.5 pg/mL; PSA: 62 pg/mL	Rat Plasma	PEDGA	[30]
Material Extrusion: FDM	Biochemical and Biophysical	Protein absorption	N/A	N/A	PLA	[31]
Material Extrusion: FDM	General: miniaturized electrochemical sensor systems	Cyclic voltammetry of redox couple standard and potentiometric pH measurements	N/A	N/A	ABS	[32]
Material Extrusion: inkjet printing-drop-on-demand printer	Biosensors manufacturing optimization	Catalytic activity and conformational changes evaluation in enzymes	N/A	N/A	PP	[33]
Material Extrusion: inkjet printing-drop-on-demand printer	Biocompatible conductive ink fabrication for neuronal sensing	Graphene patterns-based conductive inks	N/A	N/A	Graphene-PI	[34]
Material Extrusion	Food and feed quality	Mycotoxins quantification	DON: 0.07; 3-ADON: 0.10; 15-ADON: 0.06 $\mu\text{g/mL}$	Food and feed	Gelatin-Methacryloyl	[35]
Material Extrusion: FDM	Environmental: water pollution monitoring	Herbicides (atrazine and acetochlor) detection	Atrazine: 0.24 ppb; acetochlor: 3.2 ppb	Water	PLA	[36]
Material Extrusion: FDM	Environmental (water pollution monitoring) and Biomedical	Serotonin quantification in synthetic urine and catechol determination in water	Serotonin: 0.032 $\mu\text{mol/L}$; catechol: 0.26 $\mu\text{mol/L}$	Synthetic biological fluids and water	Graphene oxide-PLA	[37]

Table 1. Cont.

3D Printing Technologies	Field of Application	Analytical Purposes	Limit of Detection	Biological Sample	3D-Printed Materials	Ref.
Material Extrusion: FDM	Quality control: biofuels	Copper determination in bioethanol	0.097 µg/L	Biofuels	Carbon black-PLA	[38]
Material Extrusion: inkjet printing-direct ink writing	General: battery safety	Gas detection in lithium-ion batteries	N/A	Li-ion batteries	CuMPs-polyethylene oxide	[39]
Vat Photopolymerization	Biomedical: living biosensor	In situ monitoring of cellular metabolites	N/A	Cells	Au.pHEMA	[40]
Vat Photopolymerization	Biomedical: point-of-care (POC) diagnostics	Tumor markers (alpha-fetoprotein) detection	0.01 ng/mL	Human blood	N/A	[41]
Vat Photopolymerization	Biomedical: diabetics diagnosis	Glucose determination in human sweat and blood	25 µM	Human sweat and blood	rGO-TEPA/PB	[42]
Vat Photopolymerization	Biomedical	Glucose and cholesterol quantification in human blood	Glucose: 1.2 µM; cholesterol: 2.3 µM	Human blood	White resin	[43]
Vat Photopolymerization: SLA	Biomedical: living biosensor	Stereolithographic printing of engineered microbial in biosensor for in situ monitoring of uranium in groundwater	2.5 µM	Groundwater	PEGDa	[44]
Vat Photopolymerization: SLA	Biomedical	Metastatic cancer biomarkers quantification	DSG3: 0.10 fg/mL; VEGF-A, VEGF-C, β-Tub: 0.20 fg/mL	Human biological fluids	Chitosan	[45]
Vat Photopolymerization: SLA	Biomedical: biocompatible biosensor	Biocompatibility evaluation of commercial resins towards rat cardiomyocytes	N/A	Rat cardiomyocytes	Commercial resins	[3]
Vat Photopolymerization: digital light processing	Biomedical: cancer diagnosis	Circulating tumor cells (CTCs) detection in human blood	10 cells/mL	Human blood	PU	[46]
Vat Photopolymerization: digital light processing	Biomedical: biomarker detection in complex matrices	C-reactive protein as model biomarker	1 ng/mL	Fetal bovine serum	Plastic material (Not specified)	[47]
Vat Photopolymerization	Quality control: foods	<i>Salmonella typhimurium</i> detection in food	17 CFU/mL	Food	ABS	[48]
Vat Photopolymerization: SLA	Quality control: agri-food matrices	Antioxidant capacity (TAC) in food extracts and beverages	Gallic acid equivalent: 30 µM	Food and beverages	N/A	[49]
Vat Photopolymerization: SLA	Biophotonic technologies	3D-printed transfer molding for photonic biosensor optimization	N/A	N/A	PAMPSA-PAAm	[50]
Vat Photopolymerization: SLA	Wearable and implantable bioelectronics, robotics, energy storage, and cell cultures	Logic of architecture design applied to conductive hydrogel manufacturing	N/A	N/A	N/A	[51]
Material Jetting: Multijet technology	Biomedical: early diagnostics	Cancer metastasis monitoring	10 ⁶ cells/mL	Human biological fluids	VisiJet M3 crystal	[52]
Material Jetting: Multijet technology	Biomedical: portable-living biosensor	Cell-based biosensor for volatile compounds detection	1-octen-3-ol: 1 µM	N/A	VisiJet M2R-CL	[53]
Material Jetting: Multijet technology	Biomedical	Proteins detection	0.04 µM	Human biological fluids	VisiJet M2R-CL	[54]
Material Jetting: Multijet technology	Biomedical: aptamer-based impedimetric biosensor	<i>Escherichia coli</i> label-free detection	10 ⁵ cells/mL	Fecal material	PMMA	[55]
Material Jetting: fluid dynamic modelling	Environmental: water pollution evaluation	Freshwater toxicity monitoring	Ni(II), Cr(III): < 2 mg/L	Freshwater	N/A	[56]
Binder Jetting	Biomedical: allergy diagnosis	Immunoglobulin E detection	0.2 µg/mL	Human blood	PMMA	[57]
Powder Bed Fusion	Biomedical: point-of-care (POC) diagnostics-wearable biosensor	Real-time monitoring of electrical body signals	N/A	N/A	Sugar grains	[58]

Table 1. Cont.

3D Printing Technologies	Field of Application	Analytical Purposes	Limit of Detection	Biological Sample	3D-Printed Materials	Ref.
3D-printed modular magnetic digital microfluidic: SLA + FDM	Biomedical: point-of-care (POC) diagnostics	Biomarkers sensing, pathogen identification, antibiotic resistance determination, glucose and protein quantification	HBsAg: 61.6 ng/mL; CRP: 59.8 ng/mL; BSA: 54.6 µg/mL; glucose: 0.47 mg/dL	Human biological fluids	Clear resins/ABS	[59]
Inkjet printing + Microlithography	Bioelectronics	Quantitative comparison between microlithography and 3D printing in hydrogels manufacturing for biosensing and tissue engineering	N/A	N/A	PEDOT:PSS/ p(HEMA-co-EGMA)	[60]

2.1. Material Extrusion and Biosensors

Material extrusion 3D printing is one of the most common printing methodologies due to its simplicity of use, wide applicability, and precision. 3D printers based on an extrusion system use a screw device or a pneumatic actuator to deliver the ink through a needle or a nozzle for material deposition for the object creation. These common extrusion methods are compatible with thermoplastic materials such as PLA, ABS, PC (polycarbonate), PP (polypropylene), etc. (see Table S1, Supplementary Materials). Material deposition in X, Y, and Z axes are controlled by actuators that regulate the orientation of the nozzle in three dimensions, and each layer is built on top of the previous [16,61], tracing the printed object dimension and their design specified in the standard triangle/ file (STL), a file format extensively used for 3D printing and rapid prototyping. Amongst the 3D printing approaches based on material extrusion technology, fused deposition modelling (FDM) also known as fused filament fabrication (FFF) represents one of the most employed thanks to its ability to create complex geometries, its affordability, and simplicity to use [22,32]. In FDM, a polymer or polymer mixture, melted by a heated cartridge or a print head, is pushed through a syringe to create structures with a well-defined architecture [61]. However, this approach has some drawbacks, as the printing process is slow compared to other techniques such as stereolithography (SLA); furthermore, the quality of the printing is adequate but lower in comparison with the overall precision obtained from binder jetting and vat photopolymerization printing methods. Despite these limitations, FDM is perfectly suitable for rapid prototyping. Therefore, it is used for a wide variety of purposes, from digital healthcare and pharmaceutical applications [62] to automotive and aerospace sectors [63]. Another example of 3D ME technology is inkjet printing—a versatile technique in which electrical actuators are used to eject pico-liter volumes of liquid from micron-sized nozzles onto a substrate in a defined pattern with a layer-by-layer process. This technique is easily adaptable to a wide range of liquid materials or solid suspensions, from conductive polymers and dielectric inks to proteins and living cells with no post-processing required. Inkjet technology is efficiently exploited for the printing of paper documents, but applications in different fields such as organic electronics, sensor fabrication, chemical synthesis, and biology are reported [25,64,65]. A promising 3D technology is related to aerosol jet printing (AJP) for digital additive manufacturing at the microscale level (range from 10 µm to 100 nm). It is a direct-write additive manufacturing technique allowing for the printing of patterned circuits with high spatial resolution, avoiding the need for chemical etching. Through the use of different inks, including functional nanomaterial, AJP can be applied on different substrates, including conductors, dielectrics, semiconductors, and polymers. In some cases, consistency and reproducibility are challenging to achieve. Despite these limitations, AJP is adaptable on both 2D and 3D substrates [26,27,66]. Thus, in the last two years, all these ME 3D printing technologies have been used for biosensors or, at least, some of their components have been fabricated with applications in electrochemistry studies,

from bioelectronics applied to medical purposes [67] to environmental monitoring [68] and food safety assessment [69].

2.1.1. Material Extrusion for Biomedical Applications

Material extrusion, due to its simplicity of use and general low-cost of employment, allows the rapid prototyping of different apparatuses that can be exploited in different fields. One of the most reported in the literature is represented by biomedical applications. This paragraph gathers different examples on this topic, starting from the development of electrochemical systems suitable for healthcare monitoring. Most of electrochemical biosensors are manufactured manually; this approach inevitably leads human error. The utilization of 3D printing technologies helps to overcome these limitations, improving the properties of biosensors in terms of the conductivity and analytical performance of the system, allowing a high-throughput detection. Thus, regarding electrochemical measurements, 3D printing technology has been used to fabricate customized 3D-printed electrodes as a platform on which to develop biosensing, energy generation, and storage devices.

Marzo et al. [20] demonstrated a very interesting and innovative 3D-printed enzymatic graphene–polylactic (PLA) electrode, developed by material extrusion technology, for direct electron transfer using horseradish peroxidase enzyme for hydrogen peroxide detection. In order to confirm and facilitate heterogeneous electron transfer, gold nanoparticles were included in the system. The experimental data reported an analytical linear range of hydrogen peroxide concentration equal to 25–100 μM , and the 3D-printed electrode showed a limit of detection of 11.1 μM and a limit of quantification of 37 μM . This work creates an innovative perspective for the manufacture of third-generation electrochemical biosensors using 3D printing technology. Indeed, the utilization of graphene in 3D printing is gaining interest due to the unique properties of this material, in terms of subtlety, flexibility, and mechanical strength. Biosensors produced in this way are perfectly suitable for applications in biomedical fields (e.g., detect glucose and other biomarkers in biological fluids without using electron mediators and binder polymers), according to the needs of tailorable devices with fast and cost-reducing manufacturing features [20].

A further example of material extrusion applied to point-of-care diagnostic devices development was reported by Katseli et al. [21]. In this work, authors employed FDM 3D printing for the manufacture of an electrochemical ring (e-ring). The 3D-printed e-ring represented a wearable sensor for glucose index measured in sweat. This work was a well-conceived example of a portable POC diagnostic device, accessible in terms of costs and fabrication process. The 3D-printed components were designed using free online software, and the biosensor was thought to be accessible to a smartphone, which represents something that most people use in their daily life. The system was composed of an enduring and flexible cylindrical holder made of TPU (thermoplastic polyurethane) and three electrodes fabricated using conductive filaments, such as carbon-loaded PLA and ABS from different manufacturers. Interestingly, carbon-based PLA showed better sensitivity in glucose detection; for this reason, it was selected as material for the 3D printing of all the electrodes. An electrodeposited gold film was applied to modify the e-ring before coupling with a miniature potentiostat directly accessible by a smartphone. This device allowed for the noninvasive, nonenzymatic amperometric self-testing of glucose levels in human sweat at the concentration range of 12.5–400 $\mu\text{mol L}^{-1}$. An advantage is the absence of interference from common electroactive metabolites. The device was tested for its within-sensor reproducibility (3.4%, $n = 6$) and its long-term and mechanical stability, demonstrating solid results. The reproducibility of the sensors was calculated in terms of relative standard deviation (expressed in percentage) from measurements performed by four different devices—in this case, the value obtained was 6.8%. Both of these results demonstrated satisfactory repeatability in glucose detection and manufacturing process reproducibility. Wang et al. [22], thanks to FDM technology, overcame the crucial challenge of chiral recognition for electrochemical sensors with similar physicochemical properties such as enantiomers; in particular, the 3D-printed sensor was employed for

the chiral recognition of L and D tryptophan (Trp) in a racemic solution. Authors mixed Fe_3O_4 nanoparticles with 1,3,5-tris(p-formylphenyl)benzene and 4,4''-diamino-p-terphenyl under acidic conditions to obtain a Fe_3O_4 -magnetic covalent organic framework (COF); subsequently, they added Fe_3O_4 @COF to bovine serum albumin (BSA) as chiral surface. Lastly, they functionalized the 3D-printed nanocarbon electrode with Fe_3O_4 @COF@BSA to obtain an integrated 3D-printed nanocarbon electrode electrochemical chiral sensor, demonstrating, for the first time, the suitability of 3D printing technologies for this application. Linear sweep voltammetry was performed for the chiral recognition of the Trp isomers; the COF@BSA-functionalized 3D-printed electrode demonstrated higher efficiency in chiral recognition of L than D-Trp, and the system showed excellent repeatability for the relative quantification of the L-isomer in the racemic solution; reporting a good linearity (R^2 : 0.995) that allowed the chiral discrimination of the L-D enantiomers. This work shows potential for protein and porous material-modified 3D-printed electrodes in determining individual enantiomers in a mixture [22]. With reference to the diagnostics field, many detection technologies, such as gas chromatography or liquid chromatography coupled to mass spectrometry and enzymatic immunoassay are broadly applied to drug analysis. These analytical techniques can be very accurate and reliable, but they are time-consuming, they need sample pre-treatment, and furthermore they often require trained personnel to perform the analysis. These factors significantly limit their applications for drug analysis in clinical diagnosis [23]. To overcome these limitations, biosensors with specific features for clinical application have been developed as provided by Cheng et al. [23]. In this work the authors developed a 3D-printed portable paper cartridge using FDM technology as a portable tool for the quantitation of drug in biological fluids, such as blood, urine, and saliva for application in clinical analysis. The 3D-printed cartridge consisted of a device cover, a sampler, and a device chassis (Figure 3a,b). CAD software was used to design the structure of the object that was then manufactured by FDM 3D printer by using polylactic acid as material (Figure 3). The paper tip was finalized for samples pre-concentration. By deposition of silver nanowires at the tip, the 3D-printed paper cartridge was used for sample pre-concentration and as a surface-enhanced Raman scattering (SERS) substrate to optimize the Raman signal for quantitative analysis. Each part was rationalized in a way such that the sampler was conceived for the slow and uniform release of sample solutions, the cover with grooves was fundamental for sampler stability, and the device chassis was structured in a way to improve sample pre-concentration of the paper tip. The integrated detection protocol of the 3D-printed paper cartridge is shown in Figure 3c. The procedure was performed in three main steps: the first step was adding sample into the 3D-printed sampler; the second step involved the transfer of the sample to the hydrophilic wick of the paper tip, which is where the pre-concentration of the sample started. The advantage of this device is that the pre-concentration step occurs very quickly, with only few minutes being required, and after this period of time, the cartridge can be then removed and dried. A Raman spectroscopy was finally used to detect SERS from the cartridge. Following this procedure, each sample could be measured and quantified very rapidly. The pre-concentration capability of the cartridge significantly improved the fluorescence signal, allowing a 9.93-fold improvement in the overall SERS analysis. Compared with the multiple cooperation and multi-step methods seen in the existing technologies, this system represents a simple, cheap, and portable 3D-printed paper cartridge able to be integrated with a detection procedure within an hour. The performance of the above mentioned 3D-cartridge was evaluated by the quantitative detection of two broad spectrum anti-neoplastic drugs—epirubicin hydrochloride and cyclophosphamide—in bovine serum and artificial urine. This work presents a low-cost, portable, time-saving, 3D-printed device capable of performing the simultaneous determination of two different anticancer drugs widely used in chemotherapy, opening new perspectives on potential clinical applications [23].

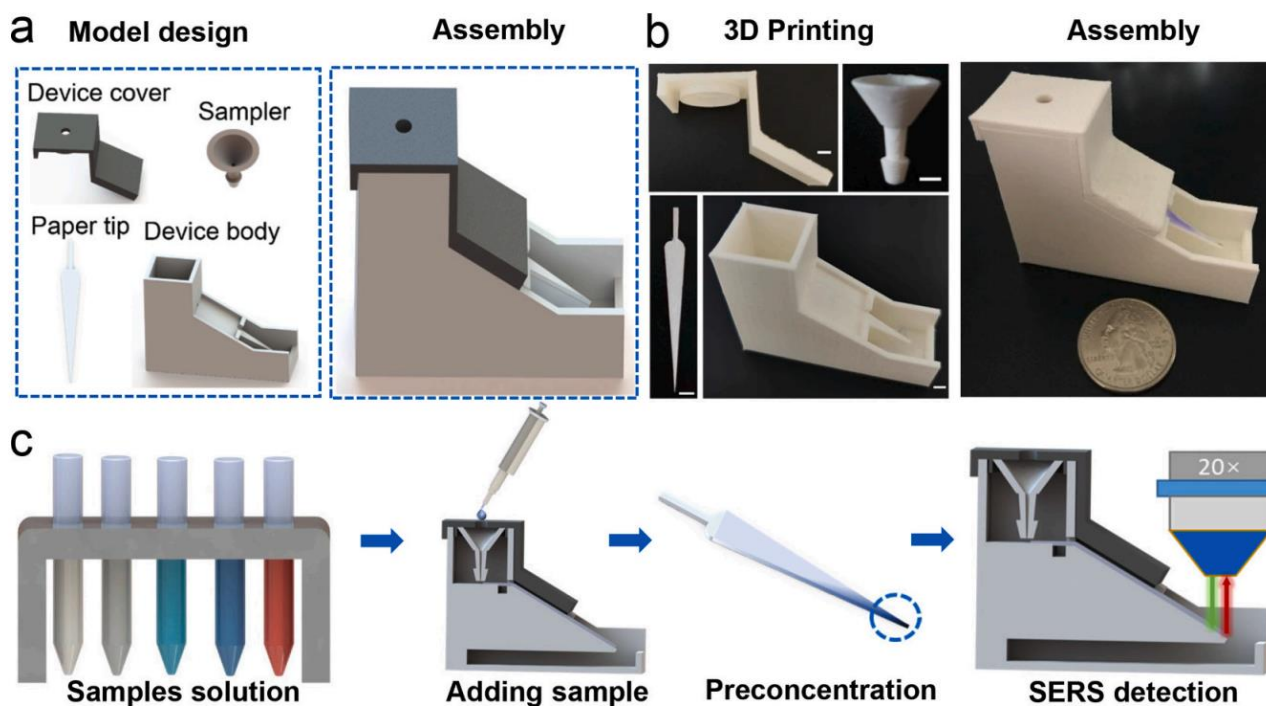


Figure 3. (a) Design schematic of 3D-printed paper cartridge. (b) Photograph of the paper cartridge's fabrication process. (Scale bars are 4 mm). (c) Integrated detection procedure of the paper cartridge. Reproduced with permission from Cheng et al. [23], *Biosensors and Bioelectronics*, 189, 113266. Published by Elsevier, 2021.

Regarding the employment of FDM technology for the manufacture of point-of-care (POC) devices, Pantazis et al. [24] developed a 3D-printed bioreactor able to perform loop-mediated isothermal amplification (LAMP) on DNA collected from saliva samples to monitor the CYP2C19 \times 2 mutation. This mutation is involved in the metabolism of the drug clopidogrel (Plavix), adopted for cardiovascular diseases treatment. The system showed significant advantages in terms of cost (less than EUR 30) and time of printing and assembly (2 h), demonstrating it to be perfectly adequate for the customized prototyping of point-of-care diagnostics. Furthermore, the ability to provide information about the safe and the effective use of a therapeutic drug to a specific person demonstrated the suitability of the device as a diagnostic system. 3D printing technologies could be exploited not only to build an ad hoc chassis and multiple elements for the device's architecture but also to produce printable biological-based ink. In the quest for innovative biomaterials for advanced therapies, hydrogels represent a natural, biocompatible, and biodegradable solution. Hydrogel scaffolds are mainly composed of polysaccharides that can be obtained from renewable and recoverable natural sources, such as algae (e.g., alginate), animals (e.g., hyaluronic acid, chitosan, and chondroitin), plants (e.g., cellulose nanocrystals pectin, starch), and microorganisms (e.g., xanthan gum, pullulan, or dextran). The chemical, physical, and biological properties of these polymers ensure their high biocompatibility, activity, and reduced enzymatic degradability. Moreover, the presence of hydroxyl, carboxyl, amino, and other hydrophilic chemical groups allows for drug interaction and a series of multiple applications [70]. As a consequence, these active materials have been used for different applications, such as regenerative medicine, drug delivery, treatment of infected wounds, and eco-friendly water purification systems [70–73]. Moreover, printable biomaterials can interact with cells by physical and chemical binding at different levels, from individual cells up to a single molecule as a function of time and system dimension [74]. In this scenario, the investigation of the interactions between living cells and biomaterials could represent a valuable tool to better understand the mechanisms behind different molecular pathways of biology. Zanotti et al. [74] investigated the adaptation of lipid the profile of

human fibroblasts to alginate 2D films and 3D-printed scaffolds. The 3D alginate scaffold was constructed using a homemade 3D printer. The alginate formulation (6% *w/v*) was printed by an extrusion process from a 26G needle in a layer-by-layer mode on the frozen printing plate ($-14\text{ }^{\circ}\text{C}$). The 3D-printed scaffold was post-processed by immersion in the in a gelling solution of CaCl_2 (3% *w/v*) or FeCl_3 (3% *w/v*) for one hour. After rinsing with deionized water, the 3D scaffolds were ready to be tested on cell culture. Before evaluating the modulation of the relative expression of lipids in dermal human fibroblasts, Zanotti et al. performed a MTT colorimetric assay to monitor the viability of cells in contact with the biomaterial. The results proved the biocompatibility of these scaffolds with cells. Here, liquid chromatography–triple quadrupole tandem mass spectrometry was used for the selected determination of the lipidomic profile of fibroblasts grown on scaffolds. Targeted markers such as, ceramides (CER), lysophosphatidylcholines (LPC), free fatty acids (FFA), and lysophosphatidic acids (LPA) were analyzed. Except for the preparation procedure, the same protocols were followed with alginate 2D films. Targeted liquid chromatography–mass spectrometry analysis revealed that different scaffolds have the capabilities to affect the relative distribution profile of the main cell membrane lipids, which could result in a variation in membrane properties related to trafficking and signaling pathways. The behavior of human fibroblasts in contact with alginate hydrogels was demonstrated to be influenced by both architectures (2D and 3D). Intriguingly, 3D geometry can add an unknown physiologically relevant aspect compared with 2D [74]. Mainly in the biosensing field, but not only, the inkjet 3D printing techniques such as direct ink writing (DIW) and drop-on-demand (DOD), have also been widely employed for the fabrication of biosensors due to their advantages of contactless printing, reduction in waste, and rapid deposition [25,33,34,39]. Inkjet printing technology has been used by Mojena-Medina et al. [25] to fabricate interdigitated-electrode sensors (IDEs) to monitor epithelial cell cultures. In particular, the inkjet-printed sensor was used for monitoring the migration, proliferation, and detachment of a monolayer of keratinocytes (HaCaT) using real-time electrochemical impedance spectroscopy (EIS). IDEs have been constructed using flexible substrates based on polyethylene terephthalate (PET); silver nanoparticles (AgNPs) were added to provide a proper conductivity and also for their self-sintering property. Despite these credits, the cytocompatibility and the chemical stability of AgNPs are not well defined. Taking this consideration into account, to fabricate sensors able to perform impedance measurements, electrodes were isolated with dielectric-based ink (SU-8); SU-8 was chosen due to its properties as insulator but also as inert material, which represents a useful feature for exposure to cell lines. Inkjet 3D printing was chosen thanks to its maskless and contactless properties and its compatibility with current bioprinting techniques. IDEs were tested to perform impedance recordings on laboratory skin tissue. Authors have found that variations in the impedance signal correlate linearly with cell density, reporting a sensitivity of $4.36\text{ cell index units/cm}^2$ with a linear regression between impedance variations and the initial value of cell density, with a coefficient of determination equal to 0.98. The relationship between impedance variations and cell status was further confirmed by fluorescence microscopy. Intriguingly, here the cell membrane was the main component affecting the total impedance. It was demonstrated that cell migration on the biosensor surface could be measured by impedance. The results obtained by monitoring this parameter were in agreement with those obtained by using the standard method based on image processing [25]. This work provides a valid alternative to monitor the in situ process associated with in vitro epidermal models for anchorage-dependent cells, skin substitutes, and tissue regeneration studies based on low-cost ink-jetted prototyping.

Finally, the use of 3D aerosol-jet-printing (AJP) technology in biosensors has been reported by Parate et al. [26], who developed an AJP graphene-based immunosensor for the simultaneous determination of two distinct cytokines in bovine serum: interferon gamma ($\text{IFN-}\gamma$) and interleukin 10 (IL-10). They selected graphene–nitrocellulose ink due to the high electrical conductivity of graphene at low thickness (nanometers scale). Using this 3D printing technology, they overcame the limit of traditional approaches used for

graphene printing, such as inkjet printing. The latter technique is linked to ink viscosity requirement properties and issues related to high-resolution printed line width, which impedes the performance of graphene-printed biosensors by some printing techniques. In the presented work, the authors optimized the aerosol jet printing process steps, obtaining an unprecedented, with regard to graphene 3D-AJP, 40 μm width line resolution of the graphene–nitrocellulose-printed electrodes. This high resolution increased the signal-to-noise ratio reported in the electrochemical characterization and, consequently, improved the electrodes' performance in cytokines detection, achieving wide sensing analytical range in serum—IFN- γ : 0.1–5 ng/mL and IL-10: 0.1–2 ng/mL; with high selectivity and low limits of detection: 25 pg/mL for IFN- γ and 46 pg/mL for IL-10. Interdigitated electrodes (IDEs) were annealed under CO₂ conditions to introduce reactive oxygen species on the graphene surface that were able to covalently link IFN- γ and IL-10 antibodies functionalized to the graphene surfaces. Moreover, these biosensors showed optimal mechanical properties, especially in terms of flexibility. The results obtained reported that AJP-printed electrochemical immunosensors were suitable for monitoring cytokines in bovine serum with wide sensing range, low detection limit, and high selectivity without the need for sample prelabeling or preconcentration [26]. Graphene-based electrodes could also be used for the detection of pathogens involved in human disease onset and for food safety assessment. Another intriguing and virtually useful daily application of the AJP technique was proposed by Ali et al. [27]. We live in a historical moment of emergency where there is a strong need for low-cost, portable, and reliable devices for the sensitive and rapid detection and early screening of disease biomarkers in the case of an outbreak. A prompt example was provided by coronavirus 2019 (COVID-19). Authors developed a nanomaterial-based biosensing device able to detect in few minutes through specific antibodies the SARS-CoV-2 spike S1 protein and its receptor binding domain. 3D nanoprinting was exploited in this work to design three-dimensional electrodes coated with nanoflakes of reduced graphene oxide in which the viral antigens were immobilized. The 3D-printed electrode was then integrated in a microfluidic device and assembled for use in a standard electrochemical cell. The antibodies were then distributed on the electrode surface, and when the viral antigens were selectively recognized, the variation in the impedance of the electrical circuit was detected. To record the signal variations a smartphone-based user-friendly interface was developed. A relevant technical aspect of the sensor is that it could be rapidly regenerated by introducing an acid solution that eluted the antibodies from the antigens, allowing subsequent analysis using the same platform. The device showed specific recognition of S1 and RBD detection; cross-reactivity and reproducibility studies were performed to assess this high sensitivity. Limits of detection reported were 2.8×10^{-15} M for the spike S1 protein and 16.9×10^{-15} M for its receptor binding domain (RBD). The explanation of this high-resolution detection capability could be attributed to the 3D architecture; the high porosity and the chemical properties of the surface's platform allowed an enhanced loading capacity of the viral antigens. The proposed sensing system could also be useful in detecting biomarkers for other infectious agents, such as Ebola, HIV, and Zika, deepening the knowledge about immune response dynamics during infections [27].

2.1.2. Material Extrusion for Biophysical Studies, Electrochemical Measurements, and Enzyme-Based Ink Development

In addition to its widespread application in healthcare monitoring, where it demonstrated a remarkable applicability, material extrusion 3D printing has also been highlighted for its suitability in other fields of application, such as biophysics, with regard to the absorption properties of relevant molecules in biochemistry and molecular biology studies. In this regard, Samarentsis et al. [31] fabricated surface plasmon resonance (SPR) and love wave (LW) surface acoustic wave (SAW) sensors for biophysical and biochemical analysis. The final goal of this device was to facilitate simultaneous measurements of optical and acoustic signals for the study of biomolecules' binding properties on a single surface. By using bovine serum albumin (BSA) as a protein model, two acoustic parameters, phase and

amplitude of a LW, were carried out in synchronization with SPR readings. Figure 4 shows the experimental set-up assembly: in addition to the SPR/LW-SAW device, the system was equipped with a plastic holder combined with a polydimethylsiloxane (PDMS) microfluidic cell so that the platform could be used in flow-through mode [31]. By using a previously designed CAD object, 3D printing technology was used here to create a device holder in PLA for the electrical connection of the sensor device with the network analyzer. In order to have a valuable acoustic signal, the pressure applied on the system's surface played a pivotal role. The specific holder incorporated miniaturized magnets, which allowed the application in each experiment of a standard pressure to the surface of the device by the flow cell. Six magnets, with diameter and thickness of 4 mm, were attached to the plastic holder by epoxy glue. The protein concentration estimated through real-time SPR measurements was reported as Γ_{SPR} , with a value equal to $125 \pm 13 \text{ ng/cm}^2$, a result comparable with previous studies reported by the authors. The developed system was the object of a systematic evaluation of optical and acoustic signals as a function of different surface perturbations, i.e., rigid mass loading (Au deposition), pure viscous loading (glycerol and sucrose solutions), and protein adsorption (BSA). The results obtained for this combined sensor set the fundamentals of future applications to other biochemical and biophysical studies, such as protein–protein and nucleic acid–protein interactions and the evaluation of surface topography influence on cell adhesion [31].

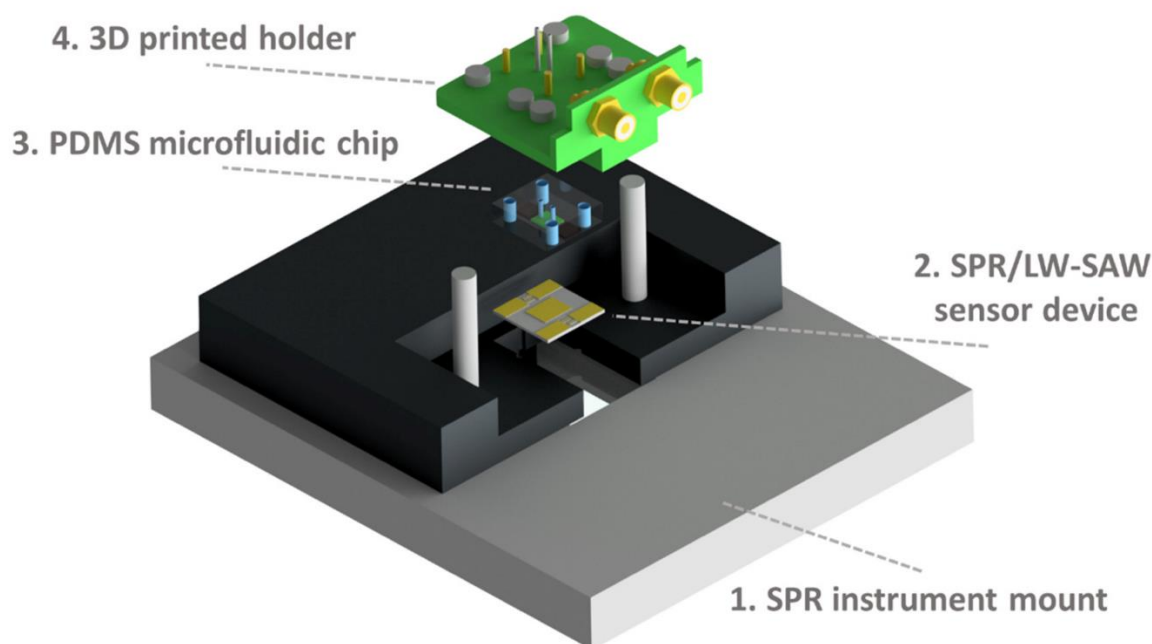


Figure 4. Experimental set-up assembly: First, the SPR/LW-SAW sensor device (2) is placed on the mount of the SPR instrument (1). Then, the PDMS chip (3) is fixed to the 3D-printed holder (4) and applied on the device surface. Reproduced with permission from Samarentsis et al. [31], *Sensors*, 20, 6177. Published by MDPI, 2020.

Deepening the possibilities offered by the FDM technology, in the wide range of diversified applications developed by this technique, it is possible to find 3D printing-based manufacturing process for the miniaturization of electrochemical devices. Miniaturization is gaining interest through the research community thanks to the increased willing to enhance the portability of diagnostic devices. This feature can, for example, allow the performance of in situ monitoring in places hard to reach with standard instrumentation. A practical example of that was reported by Sibug-Torres et al. [32]. In this work authors developed and characterized a 3D-printed $\text{Ag} | \text{AgCl} | \text{gel-KCl}$ reference electrode by fused deposition modelling that could be readily built on demand with low cost materials. These electrodes were integrated into 3D-printed miniaturized electrochemical sensor systems.

The operations for fabricating the 3D-printed reference electrode (3D-RE) are illustrated in Figure 5a. The reference electrode was assembled by two main components—the casing and the junction—both manufactured using 3D printing; the other components were readily fixed into the assembled 3D-RE body. Since the 3D-RE was designed for application in aqueous samples, they selected acrylonitrile butadiene styrene (ABS) filament as printing material for its resistance to prolonged water exposure degradation. A cross section of the 3D-RE showing the internal architecture of the electrode is reported in Figure 5b, and a picture of assembled 3D-RE is also shown in Figure 5c. A 3D-RE without a junction installed (Figure 5(c*i*)) was taken to show the internal structure of the electrode, which included an Ag|AgCl wire and agar-KCl. In the above-mentioned work, 3D printing allowed the development of porous junctions that were able to limit the leakage of the chloride ion, thus maintaining a sufficient ion conduction between the internal electrolyte layer and the sample. 3D printer parameters, such as the filament extrusion ratio, can influence the junction porosity, and thus they were used to optimize the reference electrode's potential stability and impedance. The 3D-RE developed was applied in cyclic voltammetry measurement of potassium ferricyanide and in pH sensing coupled with iridium oxide electrodeposited on a gold electrode [32]. The resulting 3D-RE was able to maintain a potential that was stable for at least 30 days under proper storage in 3M KCl. One of the most challenging parts of this work was the choice to exploit the porous property of the FFF-3D-printed materials, which is generally considered a defect, to improve the electrical properties of the reference electrode.

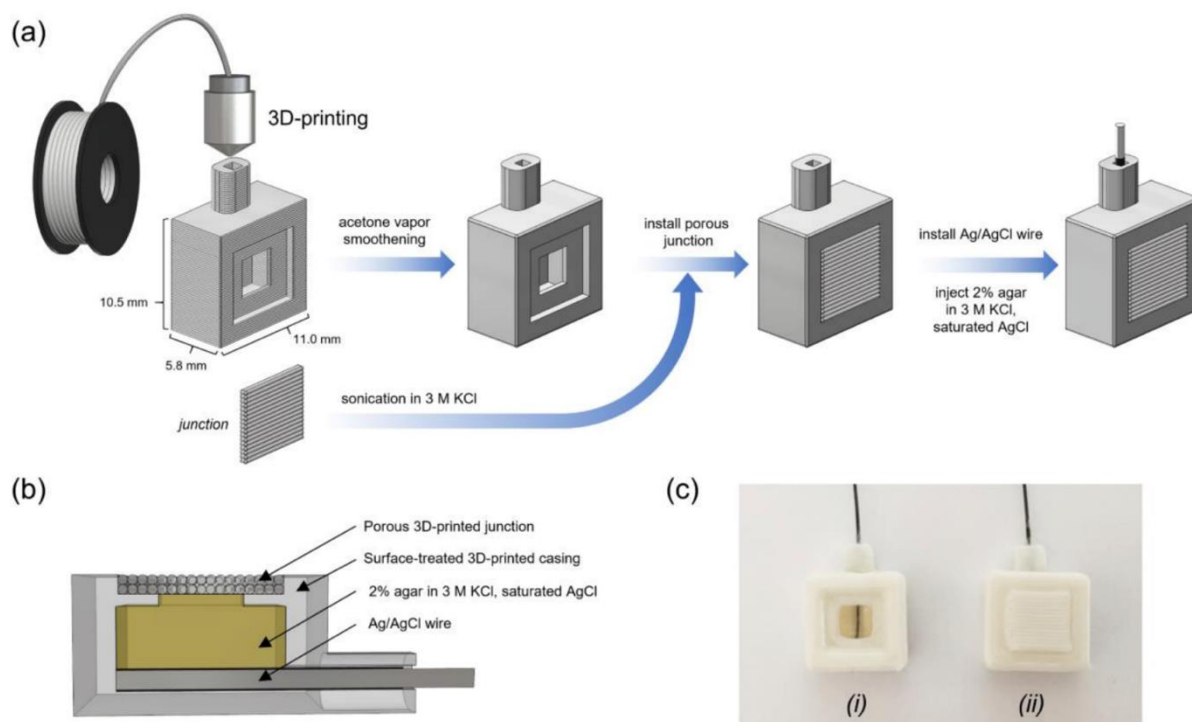


Figure 5. Design and fabrication of 3D-printed reference electrode (3D-RE). (a) Scheme illustrating the fabrication process of the 3D-RE. (b) Cross section of the 3D-RE. (c) Photograph of assembled 3D-RE (i) without a junction installed and (ii) with a junction installed. Reproduced with permission from Sibug-Torres et al. [32], *Chemosensors*, 8, 30. Published by MDPI, 2020.

An important issue that was just shallowly investigated is the overall effect of the printing process on active molecules, such as enzymes, that are added to bioink and deposited on different types of surfaces for the development of biosensors. One of the first reported studies about this intriguing topic was developed by Bai et al. [33]. In this work, authors used a piezo-driven drop-on-demand (DOD) printer to investigate the effects of pressure wave propagation exerted by inkjet printing on enzyme activity and structural

conformation. In this study, the authors measured the wave superposition, wave amplitude, resulting mechanical stress, and protein conformation change to compare the parallel printing of multiple enzymes having different sizes and structures. For the above-mentioned purpose, pyruvate oxidase, glucose oxidase, and peroxidase were employed as model enzymes. The catalytic activity of pyruvate oxidase was evaluated measuring the absorbance of quinonimine, produced from the oxidative reaction, at 550 nm. Interestingly, the mechanical stress increased the activity of pyruvate oxidase during the inkjet printing process. The mechanism behind this phenomenon was attributed to the mechanical activation or mild proteolysis that leads to variations in the three-dimensional conformation of the enzyme, improving its catalytic activity. Circular dichroism (CD) was performed on all three of the enzyme models to evaluate the eventual conformational change in the proteins during the bioprinting process; the proportion of secondary structures (α -elices and β -sheets) was more or less affected during the printing process, depending on the structural nature of the proteins. In this study, the pivotal role played by both the printing mechanism and the resulting structural and functional properties of the biomolecules involved on the final performance of the biosensor was demonstrated [33]. Asli et al. [34] presented a study where graphene was used as ink for a “drop-on-demand” 3D inkjet printer. This technology was employed in order to overcome the print instability issue relying on a time-saving process. Direct liquid phase exfoliation (DLPE) of graphite into graphene is attractive for inkjet printing, in particular for cell studies, since it was reported [75] that rat dopaminergic neuronal cells can adhere and live on graphene patterns. In this work, the authors developed a scalable and aqueous phase exfoliation method of graphite to obtain a high-quality graphene, which was employed as a tailored graphene ink with promising properties in terms of stability and electrical conductivity. The exfoliation process was based on the combination of bovine serum albumin (BSA) used as an exfoliating agent and a continuous low-speed wet-ball milling. The result of this interaction was the production of a water-dispersed graphene nanosheet. The main advantage of the printing system here described is the capability to significantly reduce graphene platelet disorientation in post-baked printed patterns with respect to commercially available inkjet printers. This means being able to minimize micro-scale junctions. These results obtained by the authors can be used as a reference guide and for further developments in the production of highly concentrated graphene and the patterning of circuits in the biosensor field [34].

2.1.3. Material Extrusion for Mycotoxins Analysis of Food and Feed

Mycotoxins are toxic compounds naturally synthesized by fungi. These secondary metabolites fit into the food chain consequent to an infection of crops, either before or after harvest, especially for cereals. When fungi find themselves to be under particular conditions in terms of humidity and temperature, they start to produce these toxic chemicals which, when undetected in food and feed, could represent a serious threat for human and animal health. To contain these harmful effects, a solid and reliable monitoring is required. In this scenario, Wei et al. [35] developed a screen-printed electrode constructed by extrusion-based 3D printing; the specific process (e.g., FDM, DoD, inkjet) was not reported. The 3D-printed electrochemical biosensors for single and multi-sample analysis were developed to study the individual and combined toxicity of three different mycotoxin models, such as deoxynivalenol (DON) and its acetylated derivatives (3-ADON and 15-ADON), providing a potential advantage over traditional analysis. The sensing capability of the biosensor was validated on a linear range of 0.1–10 ppb, 0.05–100 ppb, and 0.1–10 ppb for DON, 3-ADON, and 15-ADON, respectively, with limits of detection equal to 0.07 ppb (DON), 0.10 ppb (3-ADON), and 0.06 ppb (15-ADON). Such analytical performance is abundantly suitable with regard to the limits and regulations of mycotoxins in food and feed to safeguard consumer health and avoid foodborne diseases [76].

2.1.4. Material Extrusion Applied to Environmental Safety Monitoring

The awareness concerning the urgent need to preserve environmental safety is clear, now more than ever. 3D printing technologies demonstrate their usefulness even in this case. In the following paragraph, different applications regarding environmental safety monitoring are reported. Considering the actual widespread use of herbicides in both agriculture and gardening, the gathered data about water pollution are putting the spotlight on the environmental damage and safety issues related to the overuse and the non-optimal management of these chemicals. In this scenario, developing affordable and reliable portable devices for the detection of these pollutants is becoming increasingly urgent. In response to this need, Ruan et al. [36] employed FDM 3D printing to design a PLA-based electrochemical immunosensing system for environmental safety monitoring. In particular, they implemented a portable biosensor for the simultaneous quantification of two classes of widespread herbicides in agricultural practices: atrazine and acetochlor. FDM was selected amongst other approaches thanks to its advantages in terms of cost–reliability ratio, compared with other techniques such as SLA and inkjet printing [65]. To enhance the biosensing ability of the system, the authors coupled antibodies with palladium–platinum nanoparticles (Pd@Pt NPs), relying on the relevant catalytic activity of the latter to improve the quantitative detection of herbicides. The final architecture was called NEMEIS, which represents the acronym of nanomaterial-enhanced multiplexed electrochemical immunosensing system, which is reported in Figure 6. The device was composed of a strip cutter, a strip holder into which to plug the bifurcated immunochromatographic strip (ITS), and an electrode holder with two built-in reaction cells, with an overall size of 80 mm × 50 mm × 15 mm to obtain a system based on multiplex competitive lateral flow immunoassay (LFIA). Deepening the principle behind this device, the ITS was loaded with anti-atrazine and anti-acetochlor antibodies for the specific detection of these herbicides conjugated with mesoporous core-shell palladium@platinum nanoparticles (Ab-Pd@Pt NPs); the Pd@Pt NPs were employed for their significant peroxidase-like properties. This customized lateral-flow immunoassay enhanced the sensitivity of the analyzer, allowing the simultaneous determination of atrazine and acetochlor. The number of analytes bound on the Ab-Pd@Pt NPs was determined through electrochemical assay, measuring the general catalytic activity on the redox reaction between thionin acetate and hydrogen peroxide (H₂O₂). Pd@Pt NPs are capable of oxidizing thionine in the presence of H₂O₂, and the increased amount of the thionine oxidized form is measurable with cyclic voltammetry (CV) and differential pulse voltammetry (DPV). The peak current signal is negatively correlated with the amount of herbicides contained in the sample. Following this correlation, it is possible to determine the concentration of analytes. The NEMEIS system was based on lateral-flow immunoassay; this technique was selected due to its affordability and portability and its simplicity of usage. The data elaboration allowed the setting of a limit of detection of 0.24 ppb and 3.2 ppb for atrazine and acetochlor, respectively, in a linear range of 0.1 to 500 ppb (atrazine) and 1 to 1000 ppb (acetochlor). The limit of detection shown by the device was comparable with the value achieved with a standard method, such as HPLC for atrazine determination (0.1 ppb) and GC/MS for acetochlor (10 ppb); in addition, the analytical performance was consistent with the EU limits of herbicides in drinking water (0.5 ppb for the total amount). The valuable results obtained by this electrochemical 3D-printed biosensor unravel the wide potential of 3D-printed biosensors for different purposes, such as portable monitoring and diagnostics [36].

Silva et al. [37] reported the development of an electrochemical-based sensor for the voltametric quantification of serotonin in synthetic urine and catechol detection in artesian water, employing reduced graphene embedded into polylactic acid (rGO-PLA) for the manufacture of three different electrodes (working, pseudo-reference, and counter electrodes) printed using fused deposition modelling (FDM). In this work, the use of conductive thermoplastic filaments for 3D printing applications was evaluated for a human health and environmental survey. The 3D-printed working electrode was subsequently subjected to two sequential treatments, using nitric acid and sodium borohydride to obtain rGO-PLA

starting from graphene-PLA (G-PLA) 3D-printed electrodes. This procedure was reported to significantly improve the electrochemical properties of the final apparatus, and this experimental evidence was demonstrated by the differential-pulse-voltammetry measurement performed for serotonin detection and in tyrosinase-based voltametric analysis employed for catechol quantification in water samples. In both applications, the platform was demonstrated to be perfectly suitable for sensing and biosensing purposes, reporting a limit of detection equal to $0.032 \mu\text{mol/L}$ for serotonin quantification and $0.26 \mu\text{mol/L}$ for catechol. Particular mention should be given to the commitment that Silva et al. have shown in the development of a new procedure that avoids the use of toxic organic solvent, following the principles of green chemistry. João et al. [38] reported a manufacturing process using FDM for 3D-printed biodegradable electrodes made with carbon black/poly(lactic acid) (CB-PLA) that could be used for quality control of bioethanol fuel. The working electrode was constructed by modelling the thermoplastic conductive filament (CB-PLA) by the extruder with a hot nozzle at $220 \text{ }^\circ\text{C}$; the electrodes were 3D-printed with a hollow cube shape. The preparation of the CB-PLA 3D-printed electrode was made following this procedure: the four sides of the hollow cube were cut with scissors, giving rectangular pieces; subsequently, one side was manually polished with abrasive paper and then moistened with deionized water to control carbon black exposure; and the surface of the rectangular pieces was smoothed to avoid possible leaks when the electrode was coupled to the 3D-printed electrochemical cell. The coupling was realized by fixing the polished rectangular CB-PLA electrode over a stainless-steel plate to create a conductive surface; the electrode was then fixed using 3D-printed screw threads with a 3D-printed electrochemical cell to obtain the definitive architecture of the apparatus. The final step of fabrication involved the application of an electric potential to the electrode imbued in NaOH medium; this step was performed to remove the non-conductive polymeric material (PLA) from the working electrode surface, facilitating the electron transfer. The 3D-printed sensor was used for copper determination in bioethanol, as such metallic contaminants can be found in significant quantity in biofuels due to contamination that occurs during production, transportation, and storage. Copper ions act as a catalyst in the oxidation processes of fuel, leading to the formation of conglomerates that may obstruct motor components, such as engine pipes and injectors. The determination of copper was made using square-wave anodic-stripping voltammetry (SWASV). The 3D-printed CB-PLA electrode showed solid analytical performance in terms of limits of detection (LOD) and quantification (LOQ), with values equal to $0.097 \mu\text{g/L}$ and $0.323 \mu\text{g/L}$, respectively, in a linear range of 10 to $300 \mu\text{g/L}$. Optimal inter-day precision was reported (8%) and was calculated based on ten measurements performed on a copper concentration of $20 \mu\text{g/L}$, in addition to recovery values between 95% and 103% obtained from the copper determination of spiked samples of biofuel. Bioethanol production and commercialization depends on strict quality control. In order to produce high-quality biofuel, the development of affordable and efficient devices capable of evaluating parameters such as metallic contaminant levels is essential for promoting the reduction in greenhouse gases (GHG) linked to the combustion of fossil fuels. Lupan et al. [39] reported the use of 3D inkjet DIW technology to manufacture nanocrystalline films for sensing electrolyte vapor from lithium-ion batteries (LIBs). 3D inkjet DIW was employed for the fabrication of $\text{Al}_2\text{O}_3/\text{CuO}$ and $\text{CuO}/\text{Fe}_2\text{O}_3$ heterostructures, followed by an additional atomic layer deposition and thermal annealing step. Copper and iron nanoparticles were selected in this scenario, due to their ability to form oxide nanowires of CuO and nanoflakes of Fe_2O_3 . These two oxide metals are, respectively, *p*-type and *n*-type semiconductors. This means that they can form *p-n* junctions, which have space charge regions that are capable of detecting changes in the electronic configuration of a single constituent, making them suitable for electrolyte vapor detection. Gas response was evaluated in response to different temperature conditions; the temperature-dependent detection was not equal for all the electrolytes. The sensing properties of these 3D-DIW-printed heterostructures proved their ability to detect, in relative concentrations, common electrolyte vapors released from

LIBs. The 3D printing of nanostructures opened a new horizon in material science and nanoelectronics [39].

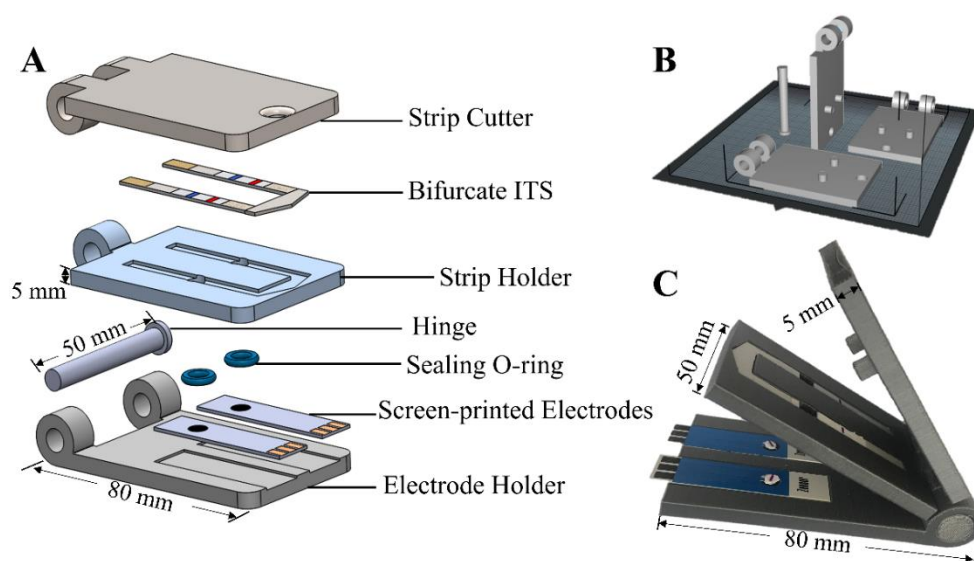


Figure 6. Prototype of the nanomaterial-enhanced multiplexed electrochemical immunosensing system (NEMEIS) device, an electrochemical immunosensing platform. Exploded view of the accessories (A), isometric 3D drawings from the top, side, and front viewpoint of the strip cutter manufactured by 3D printing (B), 3D view of assembled device, including strip cutter, strip holder with integrated strips, and electrode holder with screen-printed electrodes (C). Reproduced with permission from Ruan et al. [36], *Biosensors and Bioelectronics*, 184, 113238. Published by Elsevier, 2021.

2.2. Vat Photopolymerization and Biosensors

Vat photopolymerization (VP) or resin 3D printing is a 3D printing technique widely used in the manufacture of biosensors or their components; in particular, amongst the photopolymerization printing techniques, two VP techniques have recently gained attention for their applicability in biosensors manufacturing: stereolithography (SLA) and digital light processing (DLP) [3,7,76]. Stereolithography was patented by Chuck Hull in 1986. This method allows the realization of a 3D object by using UV light (or electron beam) to initiate a chain reaction on a layer of resin or monomer solution. The monomers are UV-sensitive and rapidly convert to polymer chains after radicalization and activation; an example of monomers involved are acrylic or epoxy-bases. After the reaction, the resin's layer is cured to sustain the following printed layers; meanwhile, a platform moves the object under processing downwards after each new layer is polymerized; finally, the unreacted resin is removed at the end of the printing process. To obtain the desired mechanical properties, heating or photo-curing, in addition to other post-process treatments, could be involved for some printed components. Using a dispersion of ceramic particles, it is possible to 3D print ceramic-based polymers. Despite the high resolution of the SLA technique, the overall process is disadvantageous in terms of time and resources. In addition, the kinetics of the reaction and the curing process show several complications. Finally, each layer has a thickness that is dependent on the energy of the light radiation and exposure. Nowadays, SLA is principally used for 3D printing of complex micro- and nanocomposites (micro-stereolithography_μSLA). DLP (digital light processing) is a 3D printing process similar to SLA, starting from a printing platform that is immersed into the resin monomers, to create the different printed parts layer by layer. The difference lies in the photopolymerization procedure. DLP uses a digital projection screen to irradiate the entire printing platform at once, curing all points at the same time. Photopolymerization techniques are arousing a considerable interest with regard to biological studies. The ease of fabrication and high printing accuracy are expanding the possibilities of using these methods in the fabrication of micro/nano-textured surfaces for cells [3,77]. A crucial parameter for the application

of commercial resins is that the mechanical properties are often inappropriate for the fabrication of electrochemical biosensors in micro-scale dimensions. Nonetheless, even considering these limitations, commercial resins are suitable for a wide range of applications thanks to their well-known characterization and advantages in terms of accessibility. As an alternative, for more flexible materials, silicones and hydrogels should be evaluated as valuable choices [3].

2.2.1. Vat Photopolymerization for High-Resolution 3D Printing of Biomedical Devices

VP 3D printing technologies can rely on their high precision of printing for the realization of complex geometries with significant accuracy. This property is reflected in the high-resolution detection capabilities of biosensors created through this 3D printing process, adding remarkable analytical properties perfectly suitable for biomedical and diagnostic purposes. Thus, in the following paragraph different examples of vat photopolymerization-based sensors are reported; in some publications (i.e., [37–40]) the specific process or printer was not specified (e.g., SLA, DLP). The first example refers to the work made by Lehman et al. [40] in developing a 3D printable plasmonic biosensor based on gold nanoparticles for in situ measurements of living cells in a non-invasive way, using a custom-built 3D printer. In this work, 2-hydroxymethylmethacrylate (HEMA) was selected as the building block for the fabrication of the sensors. Thanks to its adaptability concerning VP printing, HEMA can be employed to print complex architectures—a feature that is particularly relevant in cell-based studies. In this specific case, a polymer of HEMA (pHEMA) was embedded with gold nanoparticles (Au NPs), generating an innovative composite material acting as a plasmonic biosensor for the investigation of cell cultures and also representing a scaffold for cell adhesion, growth, and proliferation. Gold nanoparticles are well known for their numerous optical properties related to surface plasmon—specifically, AuNPs are rich in polarizable electron, which improves the interaction with electromagnetic fields. This physical properties render them extremely suitable for the analysis of biological markers via surface-enhanced Raman spectroscopy (SERS). This work showed new perspectives on the manufacture and characterization of 3D-printed materials for cell–3D scaffolds interaction studies [40]. Li et al. [41] developed a 3D printing “all-in-one” dual-modal immunoassay for the colorimetric and photoelectrochemical detection of alpha-fetoprotein (AFP), which represents a biomarker of hepatocellular carcinoma (HCC). The effort undertaken in the research of new POC diagnostic devices that can detect biomarkers such as AFP directly in human biological fluids (e.g., blood) is opening innovative opportunities in early diagnosis of cancer; 3D printing is playing a pivotal role in this process. By considering the literature dealing with the detection of AFP in biological fluids throughout the use of biosensors [78], LOD values can range from fg/mL up to several ng/mL and the whole procedure can be complex and time consuming. As a proof-of-concept, in this work a 3D-printed microreactor was employed for both the qualitative and quantitative detection of AFP. A dual-modal immunoassay system was designed with smart-management and time-saving features. Gold nanoparticle-based bioconjugate was synthesized for a first colorimetric rapid screening; this qualitative analysis of AFP had the task of rapidly discriminating the negative from the suspicious samples. The latter were subsequently analyzed for an accurate quantification using a photochemical system composed of zinc indium sulfide ($ZnIn_2S_4$), also called (ZIS), an eco-friendly semiconductor photocatalyst, which was used as a nanostructured photoactive element in a screen-printed electrode (ZIS/SPE) for the photoelectrochemical (PEC) quantification of AFP in suspicious samples, reaching an AFP limit of detection equal to 0.01 ng/mL [41].

Vat photopolymerization was also exploited for the fabrication of POC diagnostic devices of important metabolic biomolecules. In this context Cao et al. [42] developed a 3D paper-based microfluidic screen-printed electrode (SPE) composed of reduced graphene oxide-tetraethylenepentamine (rGO-TEPA/PB) employed as conductive film. A microfluidic paper-based analytical device (μ PAD) was printed by photolithography and used for quantitative detection of glucose in human sweat and blood (diabetes diagnosis); the

analytical performance reported was comparable with standard commercial glucometers, showing a limit of detection of 25 μM . Another example of 3D printing technologies that was applied to this diagnostic field was provided by Mao et al. [43]; they obtained a 3D-printed nanocomposite-based sensor array using cucurbiturils (CB), a macrocycle synthesized from acidic condensation of glycouril and formaldehyde. This supramolecule has an intriguing peroxidase-like catalytic activity, which was exploited for the colorimetric biosensing of glucose and cholesterols in blood samples, with a linear detection range from 2.5 to 250 μM for glucose quantification and 12.5 to 500 μM for cholesterol; limits of detection were 1.2 μM and 2.3 μM , respectively. A further example of a stereolithography 3D printing application in the biomedical field was successfully achieved by Dubbin et al. [44], who developed an innovative bioprinting technique to pattern microbes in three-dimensional hydrogel constructs. The authors built a stereolithographic apparatus for microbial bioprinting (SLAM Bioprinting): SLAM was capable of easily patterning engineered biofilms with small areas ($>48\text{ mm}^2$) and thickness ranging from 10 μm to $>5\text{ mm}$, with optimized control over X–Y axes that allowed a micrometer-scale resolution to be achieved. Projection micro-stereolithography (P μ SL) uses photopolymerizable resins that are deposited layer by layer to create complex 3D geometries. The authors selected this technology for the implementation of their apparatus, in order to print biofilms containing bacteria. As shown in Figure 7, SLAM bioprinting encompasses a custom-built biological P μ SL (BioP μ SL) system that used a blue LED with a 405 nm violet wavelength light radiation to project the image of the desired geometry onto a thin layer of liquid bioresin as a template for the photopolymerization. The projected light polymerized the resin into a hydrogel containing the microbes; in this way, it was possible to create a complex structure encapsulated with living bacterial cells in order to evaluate the viability and growth of printed microbial cells. Two strains of genetically modified *Escherichia coli* were selected for the printing; both strains expressed green fluorescent protein (GFP). The fluorescent signal was monitored by confocal microscopy, and the obtained results demonstrated the biocompatibility of this process (Figure 7). The visible violet wavelength was chosen for technical reasons related to the printing process (405 nm is compatible with photo-initiators) but also for its low cytotoxicity compared with shorter wavelengths (UV). As a photo-initiator in this work, the authors selected lithium phenyl-2,4,6-trimethylbenzoylphosphinate (LAP) in phosphate buffered saline (PBS); in addition, quinoline yellow (QY), a commercial yellow dye used as a food additive, was employed as a photo-absorber. Lastly, two synthetic matrices based on poly(ethylene glycol) diacrylate (PEGDa) were chosen as extracellular polymeric substance (EPS) mimicking material due to their tunability and versatility and also because previous studies successfully employed PEGDa for bacteria encapsulation. EPS are natural polymers secreted by microorganisms in their environment; these organic substances have a variable composition, even though exopolysaccharides (EPS) are the main component in bacteria. Extracellular polymeric substances are the fundamental component of biofilms, which represent an extremely relevant extracellular structure for bacterial defense, ecological fitness, and cell–cell communication. For this reason, the selection of proper synthetic matrices plays a pivotal role in the study of dynamics between microbial behavior and their three-dimensional organization. To show the efficacy of these techniques, the authors decided to investigate the ability of microbial biofilms to sense uranium. Depleted uranium is highly toxic and radioactive; for this reason, it is fundamental to build reliable sensors for the in situ monitoring of this metal. In the view of these considerations, microbial biosensors for uranium detection were developed. A modified strain of *Caulobacter crescentus* containing a transcriptionally fused vector, which allowed the bacteria to express GFP in the presence of uranium, was printed into a biofilm. The uranium-induced fluorescence was able to detect uranium in a range of concentrations equal to 2.5 to 10 μM , demonstrating the suitability of these 3D biomaterials for environmental and health safety applications. This work expands the horizons of stereolithographic (SLA) techniques, given their increasing availability in laboratory settings, showing an innovative procedure for uses ranging from microbial bioprinting to engineered biofilms manufacturing. These films

demonstrate broad applicability in different fields, including biomanufacturing, living biosensors, bioremediation, and fundamental microbiology [44].

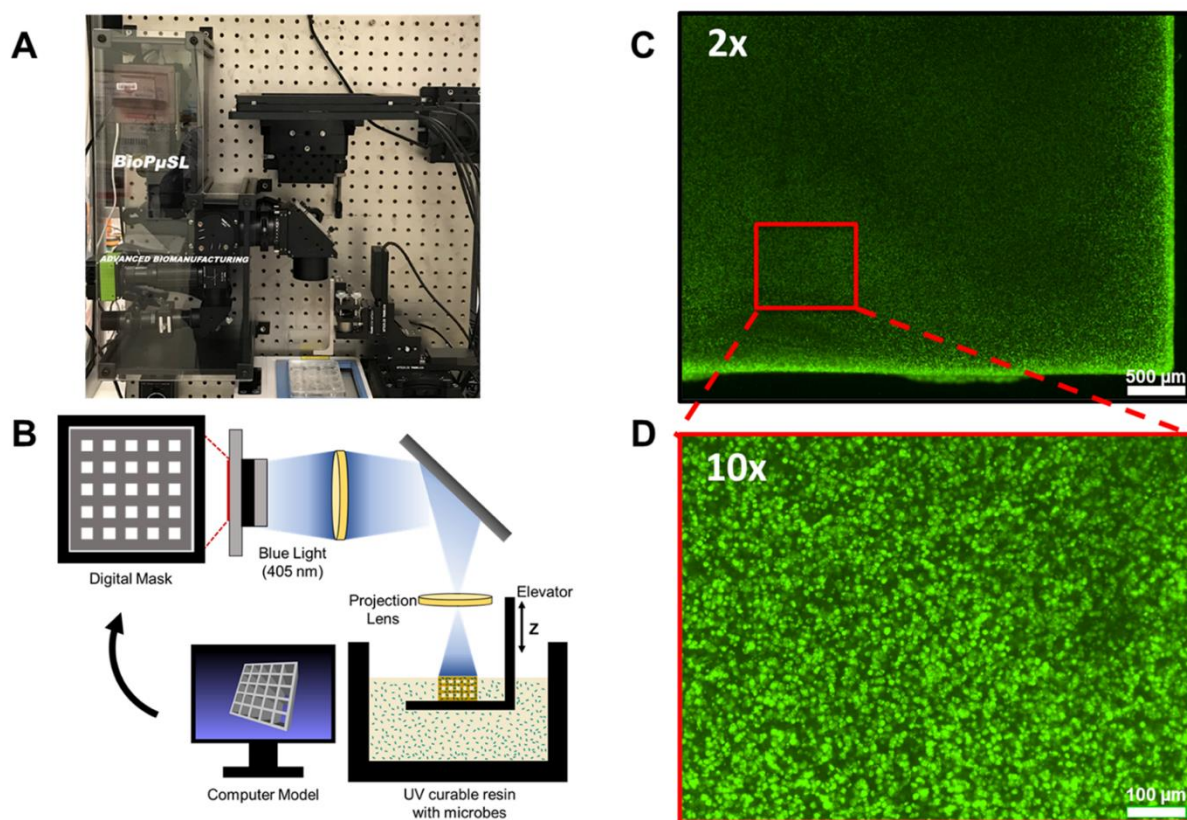


Figure 7. Demonstration of the stereolithographic apparatus for microbial (SLAM) bioprinting. Photograph of the Bio-PµSL printer used for SLAM printing (A). Schematic of the SLAM bioprinting process (B). Demonstration of the engineered biofilm using encapsulated *E. coli* expressing GFP (green) under 2× magnification (C) or 10× magnification (D). Reproduced with permission from Dubbin et al. [44], *Nano Letters*, 21, 1352–1359. Published by ACS, 2021.

A low-cost microfluidic microarray capable of lysing cells and performing a protein quantification from cell lysate was designed and 3D-printed using stereolithography, as reported by Sharafeldin et al. [45]; the 3D-printed microfluidic immunoarray was employed for the monitoring of cancer metastasis protein biomarkers, working on a single cell. This work focused on biomarkers related to head and neck squamous cell carcinoma (HNSCC); the selected protein was desmoglein 3 (DSG3) as metastatic marker, vascular endothelial growth factor (VEGF) C and D were positive controls, and β -tubulin (β -tub) was used as a loading control for the evaluation of cell number in the sample. The recognition system (detection chamber) was based on chitosan hydrogel able to swell, in contact with cell lysate, forming a 3D structure coated with immobilized antibodies. The interaction between specific antibodies and the protein biomarker was measured via chemiluminescent detection. The results demonstrated that the 3D-printed sensor was ultra-sensitive to proteins, with limits of detection of 0.10 fg/mL for DSG3 and 0.20 fg/mL for VEGF C, D, and β -tub. This work set the ground for next-generation real-time immunosensor for medical surgery, where a sample taken from a patient could be analyzed immediately for a rapid and precise in situ early diagnosis. Hart et al. [3] combined two VP technologies in order to assess the biocompatibility of different resins for 3D printing with cells. In particular, commercial resins were tested with HL-1 cells obtained from rat cardiac myocytes lines. The choice of the cell line was not random; cardiomyocytes were selected as a model of electrogenic cells due to the high rate of non-biocompatibility of commercial resins with

this particular cell type, making them perfect as a litmus test for different printable material. This investigation was extremely helpful for discovering useful insights about the proper development of fully functional and biocompatible 3D-printed biosensor devices. The wide use of biocompatible/biodegradable material, as in 3D printing, made the sensors suitable for all applications, especially those in the biomedical field, where implantation could be considered. Figure 8 shows the resin-based chip fabrication process: a digital light processing (DLP) 3D printer and stereolithography (SLA) 3D printer were tested for different commercial methacrylate-based photopolymer resins for their biocompatibility properties. Cell viability was evaluated via luminescence assay. Intriguingly, gold demonstrated a valuable viability rating, encouraging its use in electrochemical biosensors. Moreover, referring to resins, the addition of coating material such as polydimethylsiloxane (PDMS) improved the biocompatibility properties of these materials [3].

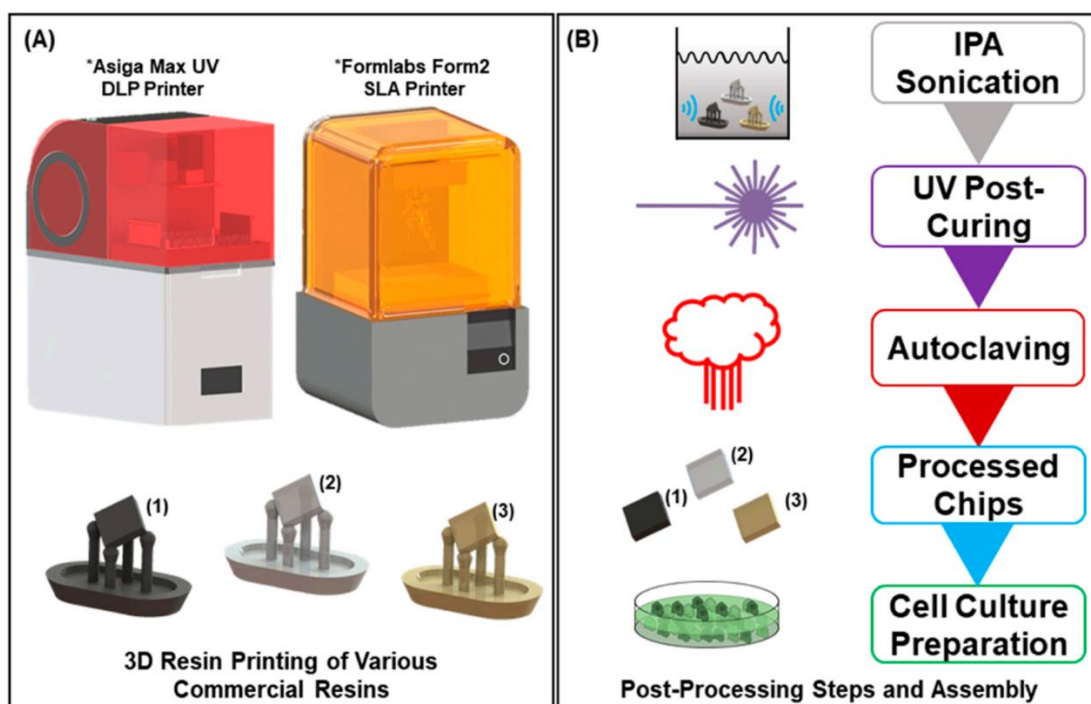


Figure 8. Resin chip fabrication: (A) schematic of the Asiga Max UV digital light processing (DLP) 3D printer and the Form2 stereolithography (SLA) 3D printer and associated printed resin chips (flexible resin in black (1), clear resin/high-temp resin in grey (2), and dental resin in brown(3)). The printer can cure many different commercial methacrylate-based photopolymer resins, allowing for a variety of sampling materials, provided that the photoinitiator absorbs between 385 and 405 nm. Each chip comes printed on a raft and support structure (as shown in the schematic) and must be singulated before post-processing. (B) Resin chip post-processing stages. Each of the indicated steps as well as the order was the final sequence used for a full regimen of resin treatment. After full post-processing, the chips can then be assembled in 48-well plates and sterilized for cell culture. Reproduced with permission from Hart et al. [3], *Biosensors*, 10, 152. Published by MDPI, 2020.

Park et al. [46] employed a digital light processing (DLP) 3D printer for the manufacture of a 3D-printed immunomagnetic concentrator (3DPIC) for ATP bioluminescence assay. This technique correlates the intracellular ATP concentration of cells with their viability, exploiting the emitted light generated from the ATP-dependent oxidation of luciferin catalyzed by luciferase. This approach was never before used for the detection of circulating tumor cells (CTCs) in blood sample, due to interferent ATP synthesized by non-CTCs. The authors developed a customized procedure of the above-mentioned assay, for the detection of CTCs using a 3D-printed immunomagnetic concentrator (3DPIC) to separate and isolate CTCs. This capability in concentrated tumor cells with high efficiency was possible thanks

to the design flexibility of 3D printing. A curve channel was designed and printed inside 3DPIC; the addition of this component reduced the flow rate of the sample, resulting in an increased cell-capturing efficiency, with a limit of detection equal to 10 cells/mL of human blood. 3DPIC allowed a rapid concentration of tumor cells, improving ATP bioluminescence assay performance, allowing for the first time the use of this technique for the detection of CTCs in a blood sample as indicators of the progression and eventual relapse of metastatic cancer. A very interesting application of 3D digital light processing for the manufacture of a microfluidic open circuit sensor system was recently presented by Sharafeldin and coworkers [47]. In this research paper, the authors customized a continuous flow 3D-printed microfluidic system for the real-time open circuit potential measurements of biomarkers in complex matrices. C-reactive protein was selected as a model molecule for the development, optimization, and validation of the quantitative biomarker assay in fetal bovine serum. Based on antibody–antigen interactions on a working electrode surface (both gold and glassy carbon electrodes were tested), excellent analytical performance was obtained in terms of baseline stability, signal repeatability, sensitivity (LOD 1 ng/mL). In particular, they demonstrated that the personalized continuous microfluidic system played a key role in reducing nonspecific absorption, improving signal-to-noise ratio and data accuracy, and reducing analysis time (less than 20 min).

2.2.2. Vat Photopolymerization and Food Safety Evaluation

Food safety is becoming a major issue for the control of food chemical and microbiological hazards; moreover, it is also involved in the commercialization of food-related goods, especially for international trade. Nowadays, more and more regulations, risk assessment methodologies, and quality standards (e.g., ISO 22000) have been established and applied to assure food safety, covering the entire supply chain, from cropping and farming to distribution. Regarding the evaluation of microbiological hazards—in particular, the detection of pathogens in food—Zheng et al. [48] fabricated an optical biosensor composed of porous gold–platinum nanocatalyst (Au@Pt NPs) coated by polyclonal antibodies and a 3D-printed fluidic chip for rapid detection of *Salmonella typhimurium*, a renowned pathogen responsible for foodborne illness. The fluidic chip was fabricated via photopolymerization, but the specific process (e.g., SLA, DLP) was not reported. The analytical performance of the system was, instead, well-described: this biosensor was able to detect *Salmonella typhimurium* in a linear range from 18 to 1.8×10^7 CFU/mL, with a LOD equal to 17 CFU/mL. *Salmonella* food safety criteria prescribe that this pathogen should not be detected in 25 g (or 10 g, depending on the food category) of food product present in the market [79]. This 3D-printed biosensor represents a sensitive, rapid, and low-cost tool for food safety evaluation, capable of overcoming traditional techniques, such as PCR and ELISA, which possess limitations in terms of time and sensitivity, respectively. The system is readily adaptable for the detection of other pathogens by changing the antibodies composition on the surface of the nanocatalyst; this flexibility brings new promising insights for the screening of pathogenic bacteria, representing a powerful tool for avoiding food poisoning [48]. Additional applications for agri-food matrices has been provided by Calabria et al. [49]: in this study, the authors developed a smartphone-based chemosensor for evaluating the total antioxidant capacity (TAC) of food extracts and beverages. TAC can be evaluated by spectrophotometric measurements of electronic transfer between the antioxidant species and free radicals; otherwise, fluorescence and chemiluminescence can be employed. These approaches require specific instrumentation, which are generally expensive and need trained personnel to perform the analysis. The presented method exploited the nucleation of gold nanoparticles (AuNPs) directed by the reducing power of an antioxidant in the presence of Au(III). The 3D-printed components of the chemosensor were fabricated by stereolithography using black-colored resins; this choice was made to avoid unwanted reflection from the light source, and the printed device was equipped with an LED-based light system to ensure optimal illumination conditions [49]. The increased concentration of Au NPs (related to the reduction driven by the antioxidant) led

to a color change in the cartridge—from colorless to red. This phenomenon allowed the correlation of the intensity of the developed color, calculated as saturation value (S), with the concentration antioxidant capacity. The colorimetric measurement was recorded with the CMOS sensor embedded in most commercial smartphones, and the captured image was then processed using freeware software (ImageJ) that easily allowed the selection of a region of interest (ROI) where the user could extrapolate the average RGB values. Applying proper calculations, it was possible to obtain a saturation value (S) that could be fitted into a calibration curve composed of S values obtained from colorimetric measurements of standard solutions with different concentrations of the antioxidant; in this work, gallic acid was used as the phenolic antioxidant standard. The quantitative determination of the samples' TAC was expressed in equivalent concentration of the corresponding antioxidant, with a limit of detection equal to 30 μM . The utilization of the CMOS image sensor embedded in a smartphone as an analytical detector for the analysis, given its cheapness and widespread global presence, highlighted the concept of the accessibility and portability of this biosensor. Braunger et al. [9] used stereolithography (SLA) to fabricate 3D-printed microfluidic devices to be used as sensors for the recognition of human taste; for this reason, the device was reported by the authors as being an electronic tongue (e-tongue). An e-tongue is a multisensory device that is able to collect data from complex liquid media, elaborating this information with computational and statistical models that lead to the association of unknown samples with specific classes, enabling their identification and distinction. In recent years, various e-tongues have been developed, also based on microfluidic devices, and a main aspect of them is the integration of passive mixers inside microchannels for studying the modulation of chemical-related effects for industrial purposes. More in depth, in this work, SLA was adopted to obtain 3D-printed staggered herringbone mixer (SHM) geometries for elastomer molding that in a second step was embedded into electronic platforms, such as printed circuit boards (PCB). The aim was to develop an automated sensor that was driven by software. The e-tongue was tested in the recognition of basic tastes (sweetness, saltiness, sourness, bitterness, and umami); for this purpose, aqueous solutions (1 mM) of sucrose, sodium chloride, chloridric acid, and glutamate were prepared and supplied to the device. The results demonstrated the ability of the 3D-printed e-tongue to elaborate data obtained from the impedance measurements of different solutions in terms of composition, at low molar concentrations. The authors exploited principal component analysis (PCA) to group different chemical compounds in relationship with human taste, also describing the modulatory effect that those substances have to each other. The experimental evidence proved that this device could be effectively commercialized as a fast, robust, and portable instrument [9].

2.2.3. Vat Photopolymerization as a Prominent tool for Biosensor Manufacturing Optimization

In this review, the high-precision of the VP 3D printing process has been strongly highlighted. Considering this parameter, it is not surprising to find well-described examples in the literature regarding the optimization of biosensors manufacturing that has exploited VP properties. About this topic, Adamopoulos et al. [50] demonstrated that high-resolution micro-stereolithography (μSLA) may be employed to fabricate silicon-based photonic systems. 3D-printed transfer molding relies on simplicity and time-saving procedures to fabricate 3D-printed microfluidic platforms with specific features in terms of components' dimensions (micro- and meso-scale) that enable integration on the platform of additional optical and electronic elements. In this way, 3D-printed transfer molding permits an increase in the adaptability of multilayer microfluidics, allowing a multiplexed approach to molecular sensing applications. A stereolithography 3D printing method was used by Jordan et al. [51] to successfully fabricate conductive hydrogels with enhanced mechanical properties and complex lattice geometry using polyaniline (PANI) as the conducting polymer. The authors customized a commercial stereolithography printer to obtain an optimized platform that was able to print hydrogels with improved elastic compress-

ibility, reduced fragility, enhanced mechanical and electrical stability through repeated cycling of usage, and remarkable compression resistance and flexibility in comparison with previously manufactured hydrogels composed of the same chemical components. The success of this process was attributed to different aspects of the production pipeline. The development of an appropriate precursor solution for the photopolymerization and the choice of the right photo-initiator were two main aspects in the printing optimization. Furthermore, increasing the stiffness of the hydrogel was pivotal for the fabrication of complex architectures. The rigidity of the printing material was enhanced, finding the right balance between the concentration of the monomer and the laser speed during the printing process. This work exploited the optimization of the structural design to overcome the limitations of chemical composition-based methods. The innovative physical properties acquired by the printed hydrogels broadened the suitability of these materials for new applications, where dynamic movement and significant structural deformations are required [51].

2.3. Material Jetting and Biosensors

Material jetting 3D printing technology applied in biosensor fabrications principally consists of MultiJet printing (MJP) that utilizes different kinds of materials (e.g., photopolymers and waxes) that are hardened when exposed to UV light, in a manner that resembles SLA. MJP's printer architecture allows material to be deposited in a line-by-line fashion; as the droplets are deposited onto the printing platform, they are immediately cured and hardened using light radiation. Material jetting can rely on its ability to print different objects in terms of mechanical properties with high resolution, even though it has its own limitation regarding printing time and accessibility [80,81]. In recent years, material jetting technology has been adopted to integrate 3D-printed microfluidics with biosensors, achieving high resolution (range of tens of microns), resulting in surface roughness of the printed device, its deformation, and resistance to harsh conditions [52–55]. Microfluidics, in fact, refers to the applied science of high-precision handling of fluids that are geometrically forced into networks of small channels, usually with micro-meter scale dimensions. This architecture allows a reduced volume of samples and reagents to be used, which represents a benefit in terms of low-cost and health and environmental safety (in the case of toxic chemicals).

2.3.1. Material Jetting 3D Printing for Healthcare Monitoring

3D printing is becoming a strictly related tool for the development of microfluidic platforms, which could be perfectly integrated in portable diagnostic sensors, such as lab-on-a-chip (LOC), microfluidic-based devices, and point-of-care diagnostics. All of these platforms are deeply employed for biomedical purposes. Evidence of this consideration was reported by Chen et al. [52], who developed MultiJet-based 3D models of microfluidic devices functionalized with anti-EpCAM (epithelial cell adhesion molecule) antibodies to isolate circulating tumor cells (CTCs) from human blood samples using specific antibodies. The microfluidic device showed some useful features, such as high surface area, fluid flow manipulation, and, thanks to its design, a considerable ability to collect tumor cells; in this study, four different kinds of EpCAM cell lines were successfully tested: three EpCAM positive (MCF-7 breast cancer, SW480 colon cancer, and PC3 prostate cancer) and one negative type (293T kidney cancer), resulting in a capture efficiency higher than 90%. The detection measurements were performed in human blood spiked with 10^6 cells/mL, exploiting the fluorescence signal emitted from the green fluorescent protein (GFP) expressed by CTCs. These results lay the foundation for the future use of 3D-printed microfluidic devices for the detection of tumor cell DNA, coupling this highly efficient capture ability with DNA-based detection techniques, such as polymerase chain reaction (PCR) and identification (DNA sequencing) in clinical diagnosis and cancer treatment [52]. Terutsuki et al. [53] employed a MultiJet printer in its maximum resolution mode for cartridge production, employing a curable and biocompatible acrylic resin as printing material. The printing process was relatively fast (approximately 4 h). The 3D-printed cartridge was structurally organized with the following design: the upper part was composed of cell cultures, an imaging-dedicated

space, and perfusion flow channels; the lower part had a sunken space dedicated to cell seeding. These two components were fixed to each other with screws and O-rings. The entire apparatus is reported in Figure 9. Intriguingly, for the investigation of the fluids' dynamic, the authors employed both computational and experimental protocols. The latter was performed using calcium imaging to monitor the flow of Or13a cells. This cell type was selected due to the expression of the odorant receptor (OR) of *Drosophila melanogaster*, and this transgenic modification allowed Or13a to be particularly sensitive to odor volatile compounds, such as 1-octen-3-ol. Analytical parameters such as detection limits, response time, and recovery values were comparable with those of commercial devices. The detection limits reported for the Or13a cells detection of 1-octen-3-ol was 1 μ M. Both procedures demonstrated the virtuosity of the cartridge system over a wide surface of action. Computational fluids dynamics (CFD) is based on a simulator software that works directly on the CAD model. Given the obtained results, the computational simulation proved to be a powerful tool for the architectural design of 3D-printed sensors. A bubble-free perfusion with a user-friendly interface and no-time-penalty manufacturing process was implemented, and the cartridge system proved to be advantageous for different cell-based bioassays and bioanalytical studies. Additionally, it can be integrated into portable biosensors, expanding their spectrum of use [53].

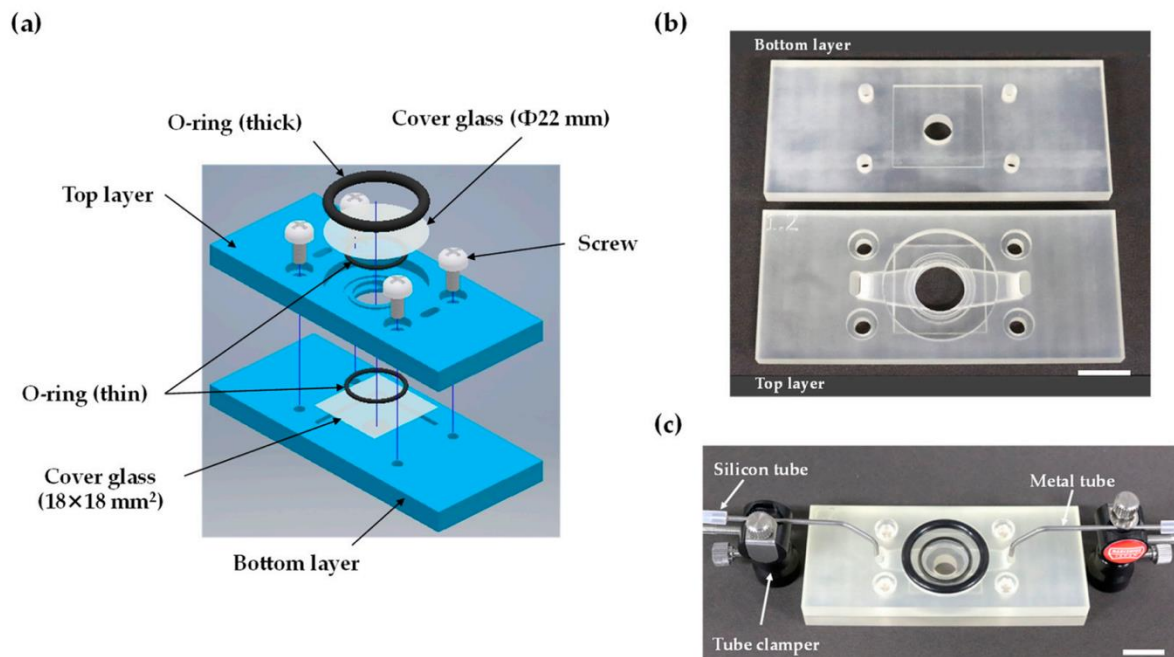


Figure 9. Design and setup of the 3D-printed perfusion cartridge system: (a) assembly view of the 3D-printed cartridge; (b) two-layer 3D-printed cartridge parts. The top layer includes flow channels and the observation area. The bottom part works as a base; (c) cartridge setup for assay buffer perfusion with metal tubes connected to silicon tubes and fixed by tube clampers. All scale bars are 10 mm. Reproduced with permission from Terutsuki et al. [53], *Sensors*, 20, 5779. Published by MDPI, 2020.

MJP technology was also applied by Graham et al. [54] to develop an integrated system that coupled microfluidics and silicon porous nanostructure-based aptasensors for label-free protein detection. In this work, a thin adhesive layer integrating a quite rough surface of 3D-printed polyacrylate microchannels with a delicate highly porous nanostructure was fabricated and successfully tested for the detection of a model target protein (D2 protein from Arabinanase family). Surface properties of 3D-printed systems can significantly influence the final analytical performance of the sensors. For this reason, a 3D multilayer system where two or more materials are used can address this issue to create more reproducible devices.

The device was able to work in a linear range from 0.25 to 18 μM , showing good selectivity and improved (about 70 fold) limit of detection (0.04 μM) compared with a non-microfluidic biosensing platform. This work paved the way for 3D printing of aptasensors for protein detection, making this process a highly valuable alternative choice to traditional methods such as PDMS-based microfluidics manufacturing coupled with soft lithography, providing evidence for future application of these 3D-printed microfluidic integrated aptasensors [54]. Siller et al. [55] involved a UV-curing process, fabricating a rigid translucent polyacrylate resin to be printed via MJP technology. Aptamers are short-sized, single-stranded DNA or RNA molecules. They can assume, thanks to intra-sequence weak interactions, three-dimensional structures (functional form); this particular 3D geometry allowed them to interact with a specific target. Thanks to specific 3D-driven interactions and also due to their physical stability and the possibility of being readily selected from a vast oligonucleotides library (SELEX techniques), aptamers represent an extraordinary tool for biosensors. In this work, the authors decided to develop aptamer-based sensors that exploited electrochemical variation in terms of impedance to detect a particular strain of *Escherichia coli*—the Crooks strain (ATCC 8739), which is a mesophilic multidrug-resistant human pathogen. The constructed 3D-printed cell systems consisted of two parts: a bottom and a top part (two exchangeable top parts were designed: one enclosing only the working electrode of the screen-printed electrode and one enclosing all electrodes). Disc magnets and the corresponding electrodes enclosing O-rings were included in the 3D-printed parts to obtain a good sealing. The device was able to sense up to 10^5 cells/mL of *E. coli* (Crooks) ($p < 0.05$), showing solid capabilities in discriminating these particular strains from others, such as *Enterococcus faecalis*. The results demonstrated the suitability of aptamer-based impedimetric biosensors for the control of foodborne disease since *E. coli* (strain Crooks) was isolated from fecal material. The presented work underlines, once again, the versatility of high-resolution 3D printing techniques for the customization of biosensors for multiple applications.

2.3.2. Material Jetting for Environmental Toxicology: Freshwater Pollutants Detection

To conclude the MJP technology list of applications on biosensors development and 3D manufacturing, an example of the employment of this technique in freshwater toxicity monitoring was reported by Agostino et al. [56]. In particular, the authors used a fluid dynamic modelling coupled with a UV-curable polymer to obtain 3D-printed electroconductive hydrogels exploited as a biosensor. In specific, the authors developed a small membraneless single chamber microbial fuel cell (MFC), which represented a biotechnological tool for transforming the chemical energy stored in organic matter into electricity through reactions catalyzed by electroactive microorganisms. The MFC-based biosensor was evaluated on the detection of a mixture of freshwater pollutants such as Ni (II) and Cr (III), showing detection capabilities at a concentration above 2 mg/L. The reported results were definitely promising, opening new perspectives on 3D-printed microbial fuel cells for environmental quality monitoring. Intriguingly, the author validated an innovative algorithm for improving data transmission and elaboration in terms of energy saving, which represents a relevant optimization for long-term data recordings. Some aspects, such as the use of 3D printing technology in the fabrication process, reduced dimensions, and the removal of the ion exchange membrane is crucial in decreasing manufacturing costs, facilitating the application of the MFC-based device in the in situ detection of water contaminants [56].

2.4. Other 3D Printing Technologies and Biosensors

In addition to the most common 3D printing techniques used in biosensing, such as material extrusion, vat photopolymerization, and material jetting, in the literature we can find further examples of 3D printing technology applications, mainly for diagnostic biosensor manufacturing [57,58]. Binder jetting (BJ), also known as the powder bed technique, is one of the technologies recognized by the ASTM standard. BJ was the first approach to 3D printing that allowed diffusion of 3D printing, following by a reduction

in printing costs. With this technology, printer heads deposit a binding agent along with colored dye onto a powder bed, fusing them layer-by-layer into a plaster construct to form a 3D construct. Interestingly, unfused powders could provide adequate support for the “overhanging” designs, and hence, simultaneous deposition of support structures is rarely required. Furthermore, it is possible to print a large variety of materials, starting from polymers—for example, PMMA powder from stainless steel to titanium to Inconel (Special Metals Corp., New Hartford, NY, USA) to tungsten carbide—and it is also possible to print using multiple colors. However, there are some limitations—for example, the final product has poor mechanical properties in terms of strength and has a poorer surface finish than stereolithography. Therefore, the post-printing reinforcement process is necessary; some materials are generally involved, such as melted wax, cyanoacrylate glue, or epoxy resin [80]. Achille et al. [57] utilized this technology to fabricate a 3D-printed microfluidic diagnostic device; particularly, up to five different binders can be printed at the same time, starting from poly(methyl methacrylate) powder as building material with an average size of 50 μm . The 3D capillarity microfluidic devices obtained from polymethyl methacrylate (PMMA) showed a high porosity when manufactured through BJ; the interstitial space was obtained during the evaporation process of the binder inside the construct. Furthermore, the functionality of the devices was achieved thanks to a precise spatial control on the surface chemistry of the pore walls. In this regard, material porosity is usually seen as a defect. Interestingly, in this particular case, the authors took advantage by exploiting the porous surface of PMMA to improve the performance of the 3D-printed microfluidic device. The fabricated systems were successfully tested in a proof-of-concept enzyme-linked immunosorbent assay, in which a multistep test timeline was completed by precisely designing capillary wetting within molded porous bodies. The ELISA assay was performed for the quantification of immunoglobulin E (IgE), the concentration rate of which is relevant for allergy diagnosis. The linear range between IgE concentration (0.2–0.8 $\mu\text{g}/\text{mL}$) and colorimetric measurements showed an R^2 equal to 0.998. The concentration range of IgE was not selected randomly: 0.2 to 0.8 $\mu\text{g}/\text{mL}$ encompasses the significant values measured for the diagnosis of allergic disease. This experimental evidence demonstrates the possibility of developing functional microfluidic 3D devices by exploiting BJ technology, with relative low costs, obviating the assembly of various components. In summary, the rapid and coherent passage between digital data and physical objects provides rapid design interactions and opens up perspectives on distributed production, proving that BJ 3D printing could represent an advantageous alternative to standard methods such as lithography [57]. Another 3D printing technology applied in biosensing is powder bed fusion (PBF), an additive manufacturing process that uses a heat source (e.g., laser, electron beam, thermal print head) to selectively consolidate material in powder form into 3D objects. The powder particles are embedded in a powder bed and heated by the heat source, which gradually indexes down as each layer is finished, so a new powder is spread over the build area. The dust particles that are thus incorporated into the printing construct ensure the integrity of the printed objects by acting as a support during the printing process, avoiding the use of additional support structures. This aspect is particularly advantageous, as with this technology it is possible to manufacture various complex and well-detailed objects that find applications in various sectors, such as the pharmaceutical sector, where for example, a pharmaceutical-grade powder blend of a drug and thermoplastic polymer (feedstock material) has been adopted. In fact, PBD technology, compared with other 3D printing processes such as material extrusion or vat photopolymerization, uses starting materials more similar to traditional tableting processes; in particular 83% of 3D-printed medical devices approved by the FDA between 2010 and 2015 were made with PBF 3D printing technology [82]. In particular, Ho et al. [58] utilized powder bed fusion as a 3D printing technique to obtain a 3D sugar scaffold for high-precision and highly sensitive wearable sensors in POC diagnostics. The fabricated biosensors showed some interesting characteristics, such as low density and substantial flexibility due to the use of 3D microcellular network-type interconnected conductive materials that were

readily printed by an inkjet head. Once a patient's body shape data were collected and 3D scanned, they were employed to fabricate on-demand personalized wearable 3D sensors for the electrochemical measurement of relevant diagnostic tests, such as electromyography (EMG), electroencephalography (EEG), and electrodermal activity (EDA) analysis, using a 3D-printed conductive electrode. These sensors demonstrated a high accuracy in the detection of actively changing body strain signals and passively changing signals, demonstrating the concrete possibility of creating tailor-made, wearable, rapid, and highly sensitive 3D sensors with real-time detection performance for monitoring rapid variations in human body signals. The described features enhanced the widespread use of reliable and accessible POC diagnostic devices in real-life applications [58]. Another example of commonly used 3D printing technologies successfully combined in biosensors production was reported by Kanitthamniyom et al. [59]. The authors presented a modular magnetic digital microfluidics (MDM) architecture that enabled rapid on-demand configuration and re-configuration of MDM platforms for customized bioanalyses in point-of-care diagnostics. In this work two different 3D printing technologies were employed to manufacture a magnetic digital microfluidics (MDM) device: stereolithography (SLA) was adopted to fabricate the baseboard of the device and all the modular components using a clear resins as materials, whereas fused deposition modeling (FDM) was involved in printing the support holder made by acrylonitrile butadiene styrene (ABS). The MDM sensor was tested on the ability to sense opportunistic pathogens such as *E. coli*, the antibiotic resistance measurement was carried out on carbapenem-resistant Enterobacteriaceae strains, biomarkers such as hepatitis B surface antigen (HBsAg), and C-reactive protein (CRP) detection using ELISA assay and glucose and protein (BSA) colorimetric quantification employing an enzymatic assay. The MDM analytical performance was valuable in all the different applications: BSA concentration was evaluated in a range from 31 to 1000 mg/mL, with a limit of detection of 54.6 µg/mL; and glucose concentration was monitored in a concentration range equal to 0.5 to 8 mg/dL, with a LOD of 0.47 mg/dL. Concerning biomarkers immunoassay quantification, the limits of detection were 61.6 ng/mL for HBsAg and 59.8 ng/mL for CRP; all of these analytical results were perfectly comparable with the performance obtained using standard instruments. The presented work showed improvement in both POC diagnostic and microfluidics-based assay applications, offering useful process strategies that can reduce costs and time in prototyping. To conclude the list of applied 3D printing technologies on biosensors production, we mention the work presented by Aggas et al. [60]. In this paper, the authors studied the potential use of poly(3,4-ethylenedioxythiophene)/polystyrene sulfonate (PEDOT/PSS) nanomaterials within poly(2-hydroxyethyl methacrylate-co-polyethylene glycol methacrylate) p(HEMA-co-EGMA) for the development of hydrogels with tunable electrical conductivity properties. Those tunable hydrogels were designed through microlithographic fabrication and 3D inkjet printing by simply adjusting their viscosity. In this work, two different hydrogel fabrication methods were compared: soft microlithography and 3D bioprint (EnvisionTEC 3D Bioplotter). Technical parameters such as printability factor and spreading rate were confronted; from this parallel confrontation, microlithography showed better performance in terms of the printability factor. Interestingly, the hydrogel's electrical properties were independent of the fabrication methods; conversely, electrochemical features showed a variation related to the PEDOT/PSS ratio (wt%). The resulting hydrogel showed good electroconductivity and biocompatibility—this last feature is pivotal for biological and medical applications [60].

3. Conclusions and Future Perspectives

Three-dimensional printing techniques are providing compelling applications in wide-ranging fields, including biosensors production, as reported by numerous previous works and confirmed by our review, which focused on the selection of publications regarding 3D printing technologies in biosensors fabrication, divulged in the last two years. We gathered recent works based on the 3D printing method used for biosensors components production

(principally relying on the AFTM standard), discussing the processes involved and presenting the main analytical purposes, achievements, and promising aspects in the so developed biosensors. In summary, the most frequently applied 3D printing technologies for biosensors fabrication were material extrusion, vat photopolymerization, and material jetting technology. All of these processes are fundamentally additive in nature and are extremely versatile for different applications in multiple fields. The possibility of conjugating single material substrates in one device allows for the rapid automatic creation of a variety of 3D biosensor prototypes slightly or significantly differing in mechanical, thermal, and electrical properties. The prototype can be subsequently improved in an easy and fast manner to increase analytical performance after testing. In general, the opportunity to tune a 3D-printed biosensor in terms of shape and materials used means that the biodegradability and robustness of the devices can be finely tuned as a function of the application. An increased robustness could be useful in improving biosensor repeatability, reducing saturation, or using the biosensor in different chemical environments. However, even if a wide range of materials can be used for 3D printing, the significant use of plastics and the biocompatibility of the final biosensors still represent an issue requiring deeper exploration and improvement. This point is stimulating both the development of printing systems that reduce the consumption of materials and the emission into the air of potentially toxic substances (i.e., nanoparticles or active chemical compounds) by improving material deposition and the development of innovative inks presenting tunable biocompatibility and biodegradability.

The versatility of 3D printing is reflected even in the fact that electrochemical biosensors have been developed for environmental, food, and biomedical applications, especially for diagnostic purposes, leading to the use of these technologies in everyday life. Practical uses of these biosensors include the rapid diagnosis of SARS-CoV-2 and further applications concerning living biosensors, but also use in water pollution monitoring, food quality control, and biofuels heavy metals determination. All of these applications demonstrate the possibility of developing 3D-printed miniaturized (microscale), highly sensitive, and generally low-cost, rapidly modifiable sensors. As a future development of 3D printing, 4D printing is representing a very promising approach, especially for the evolution of biomedical biosensors. 4D-printed objects come from a 3D printing system but are able to modify their shape or properties when exposed to external stimuli, such as pH, light, or temperature variation, etc. In the biosensor field, this means having the opportunity to develop tools with improved physiological properties for highly customizable implants for monitoring and diagnosing diseases in hard-to-reach parts of the body with a minimally invasive system. Up to now, limitations in the development of 4D printing lie in both the technology and the materials used. Even if 4D technology can be very versatile and cost effective, printing speed and resolution still need to be improved, together with the selection of biocompatible substrates.

In conclusion, we reported the continuous and intense research activity for the optimization of 3D printing procedures for the development of biosensor components and their assembly; innovation is in fact required to achieve better response speed, flexibility, and sensitivity of 3D-printed sensors in order to obtain more and more useful devices within everyone's reach, opening up a future perspective for improvements in sustainability and quality of life.

Supplementary Materials: The following supporting information can be downloaded at: <https://www.mdpi.com/article/10.3390/chemosensors10020065/s1>, Table S1: List of abbreviations related to 3D printed technologies and materials listed in Table 1 of the manuscript.

Author Contributions: Investigation, writing, and original draft preparation, G.R.; writing, review, and editing, A.Z. and L.E.; conceptualization, L.E. All authors have read and agreed to the published version of the manuscript.

Funding: This research received no external funding.

Institutional Review Board Statement: Not applicable.

Informed Consent Statement: Not applicable.

Data Availability Statement: Not applicable.

Conflicts of Interest: The authors declare no conflict of interest.

Rights and Permissions: Permission to use copyrighted materials (Figures 2–9) was obtained from formal request to authors and publishers. Licenses, where needed, were obtained via Rightslink (Copyright Clearance Center). Articles are licensed under an open access Creative Commons CC BY 4.0 license. Further permission related to the material excerpted should be directed to the publishers.

References

1. Charles, W.H. Apparatus for Production of Three-Dimensional Objects by Stereolithography. U.S. Patent 4,575,330, 11 March 1986.
2. Wang, Y.; Xu, Z.; Wu, D.; Bai, J. Current Status and Prospects of Polymer Powder 3D Printing Technologies. *Materials* **2020**, *13*, 2406. [[CrossRef](#)] [[PubMed](#)]
3. Hart, C.; Didier, C.M.; Sommerhage, F.; Rajaraman, S. Biocompatibility of Blank, Post-Processed and Coated 3D Printed Resin Structures with Electrogenic Cells. *Biosensors* **2020**, *10*, 152. [[CrossRef](#)] [[PubMed](#)]
4. Yan, Q.; Dong, H.; Su, J.; Han, J.; Song, B.; Wei, Q.; Shi, Y. A Review of 3D Printing Technology for Medical Applications. *Engineering* **2018**, *4*, 729–742. [[CrossRef](#)]
5. Palmara, G.; Frascella, F.; Roppolo, I.; Chiappone, A.; Chiadò, A. Functional 3D Printing: Approaches and Bioapplications. *Biosens. Bioelectron.* **2021**, *175*, 112849. [[CrossRef](#)]
6. Ngo, T.D.; Kashani, A.; Imbalzano, G.; Nguyen, K.T.Q.; Hui, D. Additive Manufacturing (3D Printing): A Review of Materials, Methods, Applications and Challenges. *Compos. Part B Eng.* **2018**, *143*, 172–196. [[CrossRef](#)]
7. ASTM International. *Standard Terminology for Additive Manufacturing Technologies: Designation F2792-12a*; ASTM-Standards, F2792; ASTM International: West Conshohocken, CA, USA, 2012.
8. Han, T.; Kundu, S.; Nag, A.; Xu, Y. 3D Printed Sensors for Biomedical Applications: A Review. *Sensors* **2019**, *19*, 1706. [[CrossRef](#)]
9. Braunger, M.L.; Fier, I.; Rodrigues, V.; Arratia, P.E.; Riul, A. Microfluidic Mixer with Automated Electrode Switching for Sensing Applications. *Chemosensors* **2020**, *8*, 13. [[CrossRef](#)]
10. Nagel, B.; Dellweg, H.; Gierasch, L.M. Glossary for Chemists of Terms Used in Biotechnology (IUPAC Recommendations 1992). *Pure Appl. Chem.* **1992**, *64*, 143–168. [[CrossRef](#)]
11. Fracchiolla, N.; Artuso, S.; Cortelezzi, A. Biosensors in Clinical Practice: Focus on Oncohematology. *Sensors* **2013**, *13*, 6423–6447. [[CrossRef](#)]
12. Clark, L.C.; Lyons, C. Electrode Systems For Continuous Monitoring in Cardiovascular Surgery. *Ann. N. Y. Acad. Sci.* **2006**, *102*, 29–45. [[CrossRef](#)]
13. Turner, A.P.F. Biosensors: Sense and Sensibility. *Chem. Soc. Rev.* **2013**, *42*, 3184. [[CrossRef](#)] [[PubMed](#)]
14. Bhalla, N.; Jolly, P.; Formisano, N.; Estrela, P. Introduction to Biosensors. *Essays Biochem.* **2016**, *60*, 1–8. [[CrossRef](#)]
15. Ni, Y.; Ji, R.; Long, K.; Bu, T.; Chen, K.; Zhuang, S. A Review of 3D-Printed Sensors. *Appl. Spectrosc. Rev.* **2017**, *52*, 623–652. [[CrossRef](#)]
16. Khosravani, M.R.; Reinicke, T. 3D-Printed Sensors: Current Progress and Future Challenges. *Sens. Actuators A Phys.* **2020**, *305*, 111916. [[CrossRef](#)]
17. Distler, T.; Boccaccini, A.R. 3D Printing of Electrically Conductive Hydrogels for Tissue Engineering and Biosensors—A Review. *Acta Biomater.* **2020**, *101*, 1–13. [[CrossRef](#)]
18. Sharafeldin, M.; Kadimisetty, K.; Bhalerao, K.S.; Chen, T.; Rusling, J.F. 3D-Printed Immunosensor Arrays for Cancer Diagnostics. *Sensors* **2020**, *20*, 4514. [[CrossRef](#)] [[PubMed](#)]
19. Carvalho, V.; Gonçalves, I.; Lage, T.; Rodrigues, R.O.; Minas, G.; Teixeira, S.F.C.F.; Moita, A.S.; Hori, T.; Kaji, H.; Lima, R.A. 3D Printing Techniques and Their Applications to Organ-on-a-Chip Platforms: A Systematic Review. *Sensors* **2021**, *21*, 3304. [[CrossRef](#)]
20. López Marzo, A.M.; Mayorga-Martinez, C.C.; Pumera, M. 3D-Printed Graphene Direct Electron Transfer Enzyme Biosensors. *Biosens. Bioelectron.* **2020**, *151*, 111980. [[CrossRef](#)]
21. Katseli, V.; Economou, A.; Kokkinos, C. Smartphone-Addressable 3D-Printed Electrochemical Ring for Nonenzymatic Self-Monitoring of Glucose in Human Sweat. *Anal. Chem.* **2021**, *93*, 3331–3336. [[CrossRef](#)]
22. Wang, L.; Gao, W.; Ng, S.; Pumera, M. Chiral Protein-Covalent Organic Framework 3D-Printed Structures as Chiral Biosensors. *Anal. Chem.* **2021**, *93*, 5277–5283. [[CrossRef](#)]
23. Cheng, H.; Yi, L.; Wu, J.; Li, G.; Zhao, G.; Xiao, Z.; Hu, B.; Zhao, L.; Tian, J. Drug Preconcentration and Direct Quantification in Biofluids Using 3D-Printed Paper Cartridge. *Biosens. Bioelectron.* **2021**, *189*, 113266. [[CrossRef](#)] [[PubMed](#)]
24. Pantazis, A.K.; Papadakis, G.; Parasyris, K.; Stavrinidis, A.; Gizeli, E. 3D-Printed Bioreactors for DNA Amplification: Application to Companion Diagnostics. *Sens. Actuators B Chem.* **2020**, *319*, 128161. [[CrossRef](#)]
25. Mojena-Medina, D.; Hubl, M.; Bäuscher, M.; Jorcano, J.L.; Ngo, H.-D.; Acedo, P. Real-Time Impedance Monitoring of Epithelial Cultures with Inkjet-Printed Interdigitated-Electrode Sensors. *Sensors* **2020**, *20*, 5711. [[CrossRef](#)]

26. Parate, K.; Rangnekar, S.V.; Jing, D.; Mendivelso-Perez, D.L.; Ding, S.; Secor, E.B.; Smith, E.A.; Hostetter, J.M.; Hersam, M.C.; Claussen, J.C. Aerosol-Jet-Printed Graphene Immunosensor for Label-Free Cytokine Monitoring in Serum. *ACS Appl. Mater. Interfaces* **2020**, *12*, 8592–8603. [[CrossRef](#)]
27. Ali, M.A.; Hu, C.; Jahan, S.; Yuan, B.; Saleh, M.S.; Ju, E.; Gao, S.; Panat, R. Sensing of COVID-19 Antibodies in Seconds via Aerosol Jet Nanoprinted Reduced-Graphene-Oxide-Coated 3D Electrodes. *Adv. Mater.* **2021**, *33*, 2006647. [[CrossRef](#)] [[PubMed](#)]
28. Contreras-Naranjo, J.E.; Perez-Gonzalez, V.H.; Mata-Gómez, M.A.; Aguilar, O. 3D-Printed Hybrid-Carbon-Based Electrodes for Electroanalytical Sensing Applications. *Electrochem. Commun.* **2021**, *130*, 107098. [[CrossRef](#)]
29. Crevillen, A.G.; Mayorga-Martinez, C.C.; Zelenka, J.; Rimpelová, S.; Ruml, T.; Pumera, M. 3D-Printed Transmembrane Glycoprotein Cancer Biomarker Aptasensor. *Appl. Mater. Today* **2021**, *24*, 101153. [[CrossRef](#)]
30. He, Z.; Huffman, J.; Curtin, K.; Garner, K.L.; Bowdridge, E.C.; Li, X.; Nurkiewicz, T.R.; Li, P. Composable Microfluidic Plates (CPlate): A Simple and Scalable Fluid Manipulation System for Multiplexed Enzyme-Linked Immunosorbent Assay (ELISA). *Anal. Chem.* **2021**, *93*, 1489–1497. [[CrossRef](#)]
31. Samarentsis, A.G.; Pantazis, A.K.; Tsortos, A.; Friedt, J.-M.; Gizeli, E. Hybrid Sensor Device for Simultaneous Surface Plasmon Resonance and Surface Acoustic Wave Measurements. *Sensors* **2020**, *20*, 6177. [[CrossRef](#)]
32. Sibug-Torres, S.M.; Go, L.P.; Enriquez, E.P. Fabrication of a 3D-Printed Porous Junction for Ag|AgCl|gel-KCl Reference Electrode. *Chemosensors* **2020**, *8*, 130. [[CrossRef](#)]
33. Bai, Y.; Zhang, D.; Guo, Q.; Xiao, J.; Zheng, M.; Yang, J. Study of the Enzyme Activity Change Due to Inkjet Printing for Biosensor Fabrication. *ACS Biomater. Sci. Eng.* **2021**, *7*, 787–793. [[CrossRef](#)] [[PubMed](#)]
34. Niaraki Asli, A.E.; Guo, J.; Lai, P.L.; Montazami, R.; Hashemi, N.N. High-Yield Production of Aqueous Graphene for Electrohydrodynamic Drop-on-Demand Printing of Biocompatible Conductive Patterns. *Biosensors* **2020**, *10*, 6. [[CrossRef](#)] [[PubMed](#)]
35. Wei, K.; Sun, J.; Gao, Q.; Yang, X.; Ye, Y.; Ji, J.; Sun, X. 3D “Honeycomb” Cell/Carbon Nanofiber/Gelatin Methacryloyl (GelMA) Modified Screen-Printed Electrode for Electrochemical Assessment of the Combined Toxicity of Deoxynivalenol Family Mycotoxins. *Bioelectrochemistry* **2021**, *139*, 107743. [[CrossRef](#)] [[PubMed](#)]
36. Ruan, X.; Wang, Y.; Kwon, E.Y.; Wang, L.; Cheng, N.; Niu, X.; Ding, S.; Van Wie, B.J.; Lin, Y.; Du, D. Nanomaterial-Enhanced 3D-Printed Sensor Platform for Simultaneous Detection of Atrazine and Acetochlor. *Biosens. Bioelectron.* **2021**, *184*, 113238. [[CrossRef](#)]
37. Silva, V.A.O.P.; Fernandes-Junior, W.S.; Rocha, D.P.; Stefano, J.S.; Munoz, R.A.A.; Bonacin, J.A.; Janegitz, B.C. 3D-Printed Reduced Graphene Oxide/Poly(lactic Acid) Electrodes: A New Prototyped Platform for Sensing and Biosensing Applications. *Biosens. Bioelectron.* **2020**, *170*, 112684. [[CrossRef](#)]
38. João, A.F.; Squizzato, A.L.; Richter, E.M.; Muñoz, R.A.A. Additive-Manufactured Sensors for Biofuel Analysis: Copper Determination in Bioethanol Using a 3D-Printed Carbon Black/Poly(lactic Acid) Electrode. *Anal. Bioanal. Chem.* **2020**, *412*, 2755–2762. [[CrossRef](#)] [[PubMed](#)]
39. Lupan, O.; Krüger, H.; Siebert, L.; Ababii, N.; Kohlmann, N.; Buzdugan, A.; Bodduluri, M.T.; Magariu, N.; Terasa, M.-I.; Strunskus, T.; et al. Additive Manufacturing as a Means of Gas Sensor Development for Battery Health Monitoring. *Chemosensors* **2021**, *9*, 252. [[CrossRef](#)]
40. Lehman, S.E.; McCracken, J.M.; Miller, L.A.; Jayalath, S.; Nuzzo, R.G. Biocompliant Composite Au/PHEMA Plasmonic Scaffolds for 3D Cell Culture and Noninvasive Sensing of Cellular Metabolites. *Adv. Healthc. Mater.* **2021**, *10*, 2001040. [[CrossRef](#)]
41. Li, X.; Pan, X.; Lu, J.; Zhou, Y.; Gong, J. Dual-Modal Visual/Photoelectrochemical All-in-One Bioassay for Rapid Detection of AFP Using 3D Printed Microreactor Device. *Biosens. Bioelectron.* **2020**, *158*, 112158. [[CrossRef](#)]
42. Cao, L.; Han, G.-C.; Xiao, H.; Chen, Z.; Fang, C. A Novel 3D Paper-Based Microfluidic Electrochemical Glucose Biosensor Based on RGO-TEPA/PB Sensitive Film. *Anal. Chim. Acta* **2020**, *1096*, 34–43. [[CrossRef](#)]
43. Mao, D.; Li, W.; Zhang, F.; Yang, S.; Isak, A.N.; Song, Y.; Guo, Y.; Cao, S.; Zhang, R.; Feng, C.; et al. Nanocomposite of Peroxidase-Like Cucurbit[6]Urils with Enzyme-Encapsulated ZIF-8 and Application for Colorimetric Biosensing. *ACS Appl. Mater. Interfaces* **2021**, *13*, 39719–39729. [[CrossRef](#)] [[PubMed](#)]
44. Dubbin, K.; Dong, Z.; Park, D.M.; Alvarado, J.; Su, J.; Wasson, E.; Robertson, C.; Jackson, J.; Bose, A.; Moya, M.L.; et al. Projection Microstereolithographic Microbial Bioprinting for Engineered Biofilms. *Nano Lett.* **2021**, *21*, 1352–1359. [[CrossRef](#)] [[PubMed](#)]
45. Sharafeldin, M.; Chen, T.; Ozkaya, G.U.; Choudhary, D.; Molinolo, A.A.; Gutkind, J.S.; Rusling, J.F. Detecting Cancer Metastasis and Accompanying Protein Biomarkers at Single Cell Levels Using a 3D-Printed Microfluidic Immunoarray. *Biosens. Bioelectron.* **2021**, *171*, 112681. [[CrossRef](#)] [[PubMed](#)]
46. Park, C.; Abafogi, A.T.; Ponnuruvelu, D.V.; Song, I.; Ko, K.; Park, S. Enhanced Luminescent Detection of Circulating Tumor Cells by a 3D Printed Immunomagnetic Concentrator. *Biosensors* **2021**, *11*, 278. [[CrossRef](#)]
47. Sharafeldin, M.; James, T.; Davis, J.J. Open Circuit Potential as a Tool for the Assessment of Binding Kinetics and Reagentless Protein Quantitation. *Anal. Chem.* **2021**, *93*, 14748–14754. [[CrossRef](#)]
48. Zheng, L.; Cai, G.; Qi, W.; Wang, S.; Wang, M.; Lin, J. Optical Biosensor for Rapid Detection of *Salmonella Typhimurium* Based on Porous Gold@Platinum Nanocatalysts and a 3D Fluidic Chip. *ACS Sens.* **2020**, *5*, 65–72. [[CrossRef](#)]
49. Calabria, D.; Guardigli, M.; Severi, P.; Trozzi, I.; Pace, A.; Cinti, S.; Zangheri, M.; Mirasoli, M. A Smartphone-Based Chemosensor to Evaluate Antioxidants in Agri-Food Matrices by In Situ AuNP Formation. *Sensors* **2021**, *21*, 5432. [[CrossRef](#)]
50. Adamopoulos, C.; Gharia, A.; Niknejad, A.; Stojanović, V.; Anwar, M. Microfluidic Packaging Integration with Electronic-Photonic Biosensors Using 3D Printed Transfer Molding. *Biosensors* **2020**, *10*, 177. [[CrossRef](#)]

51. Jordan, R.S.; Frye, J.; Hernandez, V.; Prado, I.; Giglio, A.; Abbasizadeh, N.; Flores-Martinez, M.; Shirzad, K.; Xu, B.; Hill, I.M.; et al. 3D Printed Architected Conducting Polymer Hydrogels. *J. Mater. Chem. B* **2021**, *9*, 7258–7270. [[CrossRef](#)]
52. Chen, J.; Liu, C.-Y.; Wang, X.; Sweet, E.; Liu, N.; Gong, X.; Lin, L. 3D Printed Microfluidic Devices for Circulating Tumor Cells (CTCs) Isolation. *Biosens. Bioelectron.* **2020**, *150*, 111900. [[CrossRef](#)]
53. Terutsuki, D.; Mitsuno, H.; Kanzaki, R. 3D-Printed Bubble-Free Perfusion Cartridge System for Live-Cell Imaging. *Sensors* **2020**, *20*, 5779. [[CrossRef](#)] [[PubMed](#)]
54. Arshavsky-Graham, S.; Enders, A.; Ackerman, S.; Bahnmann, J.; Segal, E. 3D-Printed Microfluidics Integrated with Optical Nanostructured Porous Aptasensors for Protein Detection. *Microchim. Acta* **2021**, *188*, 67. [[CrossRef](#)] [[PubMed](#)]
55. Siller, I.G.; Preuss, J.-A.; Urmann, K.; Hoffmann, M.R.; Scheper, T.; Bahnmann, J. 3D-Printed Flow Cells for Aptamer-Based Impedimetric Detection of *E. Coli* Crooks Strain. *Sensors* **2020**, *20*, 4421. [[CrossRef](#)] [[PubMed](#)]
56. Agostino, V.; Massaglia, G.; Gerosa, M.; Sacco, A.; Saracco, G.; Margaria, V.; Quaglio, M. Environmental Electroactive Consortia as Reusable Biosensing Element for Freshwater Toxicity Monitoring. *New Biotechnol.* **2020**, *55*, 36–45. [[CrossRef](#)]
57. Achille, C.; Parra-Cabrera, C.; Dochy, R.; Ordutowski, H.; Piovesan, A.; Piron, P.; Van Looy, L.; Kushwaha, S.; Reynaerts, D.; Verboven, P.; et al. 3D Printing of Monolithic Capillarity-Driven Microfluidic Devices for Diagnostics. *Adv. Mater.* **2021**, *33*, 2008712. [[CrossRef](#)]
58. Ho, D.H.; Hong, P.; Han, J.T.; Kim, S.; Kwon, S.J.; Cho, J.H. 3D-Printed Sugar Scaffold for High-Precision and Highly Sensitive Active and Passive Wearable Sensors. *Adv. Sci.* **2020**, *7*, 1902521. [[CrossRef](#)]
59. Kanitthamniyom, P.; Zhou, A.; Feng, S.; Liu, A.; Vasoo, S.; Zhang, Y. A 3D-Printed Modular Magnetic Digital Microfluidic Architecture for on-Demand Bioanalysis. *Microsyst. Nanoeng.* **2020**, *6*, 48. [[CrossRef](#)]
60. Aggas, J.R.; Abasi, S.; Phipps, J.F.; Podstawczyk, D.A.; Guiseppi-Elie, A. Microfabricated and 3-D Printed Electroconductive Hydrogels of PEDOT:PSS and Their Application in Bioelectronics. *Biosens. Bioelectron.* **2020**, *168*, 112568. [[CrossRef](#)]
61. Placone, J.K.; Engler, A.J. Recent Advances in Extrusion-Based 3D Printing for Biomedical Applications. *Adv. Healthc. Mater.* **2018**, *7*, 1701161. [[CrossRef](#)]
62. Awad, A.; Trenfield, S.J.; Gaisford, S.; Basit, A.W. 3D Printed Medicines: A New Branch of Digital Healthcare. *Int. J. Pharm.* **2018**, *548*, 586–596. [[CrossRef](#)]
63. Ferretti, P.; Santi, G.M.; Leon-Cardenas, C.; Freddi, M.; Donnici, G.; Frizziero, L.; Liverani, A. Molds with Advanced Materials for Carbon Fiber Manufacturing with 3D Printing Technology. *Polymers* **2021**, *13*, 3700. [[CrossRef](#)] [[PubMed](#)]
64. Napadensky, E. Inkjet 3D Printing. In *The Chemistry of Inkjet Inks*; World Scientific: Singapore, 2009; p. 255. ISBN 978-981-281-821-828.
65. Delaney, J.T.; Smith, P.J.; Schubert, U.S. Inkjet Printing of Proteins. *Soft Matter* **2009**, *5*, 4866. [[CrossRef](#)]
66. Secor, E.B. Principles of Aerosol Jet Printing. *Flex. Print. Electron.* **2018**, *3*, 035002. [[CrossRef](#)]
67. Aimar, A.; Palermo, A.; Innocenti, B. The Role of 3D Printing in Medical Applications: A State of the Art. *J. Healthc. Eng.* **2019**, *2019*, 1–10. [[CrossRef](#)]
68. Nadagouda, M.N.; Ginn, M.; Rastogi, V. A Review of 3D Printing Techniques for Environmental Applications. *Curr. Opin. Chem. Eng.* **2020**, *28*, 173–178. [[CrossRef](#)] [[PubMed](#)]
69. Liu, Z.; Zhang, Y.; Xu, S.; Zhang, H.; Tan, Y.; Ma, C.; Song, R.; Jiang, L.; Yi, C. A 3D Printed Smartphone Optosensing Platform for Point-of-Need Food Safety Inspection. *Anal. Chim. Acta* **2017**, *966*, 81–89. [[CrossRef](#)] [[PubMed](#)]
70. Pushpamalar, J.; Meganathan, P.; Tan, H.L.; Dahlan, N.A.; Ooi, L.-T.; Neerooa, B.N.H.M.; Essa, R.Z.; Shameli, K.; Teow, S.-Y. Development of a Polysaccharide-Based Hydrogel Drug Delivery System (DDS): An Update. *Gels* **2021**, *7*, 153. [[CrossRef](#)]
71. Bergonzi, C.; Bianchera, A.; Remaggi, G.; Ossiprandi, M.C.; Zimetti, F.; Marchi, C.; Bernini, F.; Bettini, R.; Elviri, L. Biocompatible 3D Printed Chitosan-Based Scaffolds Containing α -Tocopherol Showing Antioxidant and Antimicrobial Activity. *Appl. Sci.* **2021**, *11*, 7253. [[CrossRef](#)]
72. Bergonzi, C.; Remaggi, G.; Graiff, C.; Bergamonti, L.; Potenza, M.; Ossiprandi, M.C.; Zanotti, I.; Bernini, F.; Bettini, R.; Elviri, L. Three-Dimensional (3D) Printed Silver Nanoparticles/Alginate/Nanocrystalline Cellulose Hydrogels: Study of the Antimicrobial and Cytotoxicity Efficacy. *Nanomaterials* **2020**, *10*, 844. [[CrossRef](#)] [[PubMed](#)]
73. Bergamonti, L.; Bergonzi, C.; Graiff, C.; Lottici, P.P.; Bettini, R.; Elviri, L. 3D Printed Chitosan Scaffolds: A New TiO₂ Support for the Photocatalytic Degradation of Amoxicillin in Water. *Water Res.* **2019**, *163*, 114841. [[CrossRef](#)]
74. Zanotti, I.; Marando, S.; Remaggi, G.; Bergonzi, C.; Bernini, F.; Bettini, R.; Elviri, L. The Adaptation of Lipid Profile of Human Fibroblasts to Alginate 2D Films and 3D Printed Scaffolds. *Biochim. Biophys. Acta (BBA) Gen. Subj.* **2021**, *1865*, 129734. [[CrossRef](#)] [[PubMed](#)]
75. Guo; Niaraki Asli; Williams; Lai; Wang; Montazami; Hashemi Viability of Neural Cells on 3D Printed Graphene Bioelectronics. *Biosensors* **2019**, *9*, 112. [[CrossRef](#)] [[PubMed](#)]
76. Mazumder, P.M.; Sasmal, D. Mycotoxins—Limits and Regulations. *Anc. Sci. Life* **2001**, *20*, 1–19.
77. Zhao, Z.; Tian, X.; Song, X. Engineering Materials with Light: Recent Progress in Digital Light Processing Based 3D Printing. *J. Mater. Chem. C* **2020**, *8*, 13896–13917. [[CrossRef](#)]
78. Mohammadinejad, A.; Kazemi Oskuee, R.; Eivazzadeh-Keihan, R.; Rezayi, M.; Baradaran, B.; Maleki, A.; Hashemzaei, M.; Mokhtarzadeh, A.; de la Guardia, M. Development of Biosensors for Detection of Alpha-Fetoprotein: As a Major Biomarker for Hepatocellular Carcinoma. *TrAC Trends Anal. Chem.* **2020**, *130*, 115961. [[CrossRef](#)]
79. European Food Safety Authority. European Centre for Disease Prevention and Control The European Union One Health 2019 Zoonoses Report. *EFS2 J.* **2021**, *19*, e05926. [[CrossRef](#)]

80. Chae, M.P.; Rozen, W.M.; McMenamin, P.G.; Findlay, M.W.; Spychal, R.T.; Hunter-Smith, D.J. Emerging Applications of Bedside 3D Printing in Plastic Surgery. *Front. Surg.* **2015**, *2*, 25. [[CrossRef](#)]
81. Yoo, S.-Y.; Kim, S.-K.; Heo, S.-J.; Koak, J.-Y.; Kim, J.-G. Dimensional Accuracy of Dental Models for Three-Unit Prostheses Fabricated by Various 3D Printing Technologies. *Materials* **2021**, *14*, 1550. [[CrossRef](#)]
82. Awad, A.; Fina, F.; Goyanes, A.; Gaisford, S.; Basit, A.W. Advances in Powder Bed Fusion 3D Printing in Drug Delivery and Healthcare. *Adv. Drug Deliv. Rev.* **2021**, *174*, 406–424. [[CrossRef](#)]